



## **FHL1 is a major host factor for chikungunya virus infection**

Laurent Meertens, Mohamed Lamine Hafirassou, Thérèse Couderc, Lucie Bonnet-Madin, Vasiliya Kril, Beate Mareike Kümmerer, Athena Labeau, Alexis Brugier, Etienne Simon-Loriere, Julien Burlaud-Gaillard, et al.

### **► To cite this version:**

Laurent Meertens, Mohamed Lamine Hafirassou, Thérèse Couderc, Lucie Bonnet-Madin, Vasiliya Kril, et al.. FHL1 is a major host factor for chikungunya virus infection. *Nature*, 2019, 574 (7777), pp.259-263. 10.1038/s41586-019-1578-4 . inserm-02355424v2

**HAL Id: inserm-02355424**

**<https://inserm.hal.science/inserm-02355424v2>**

Submitted on 9 Feb 2023

**HAL** is a multi-disciplinary open access archive for the deposit and dissemination of scientific research documents, whether they are published or not. The documents may come from teaching and research institutions in France or abroad, or from public or private research centers.

L'archive ouverte pluridisciplinaire **HAL**, est destinée au dépôt et à la diffusion de documents scientifiques de niveau recherche, publiés ou non, émanant des établissements d'enseignement et de recherche français ou étrangers, des laboratoires publics ou privés.



Distributed under a Creative Commons Attribution - NonCommercial 4.0 International License

# **FHL1 is a major host factor for chikungunya virus infection**

Laurent Meertens<sup>1#\*</sup>, Mohamed Lamine Hafirassou<sup>1</sup>, Therese Couderc<sup>2</sup>, Lucie Bonnet-Madin<sup>1</sup>, Vasiliya Kril<sup>1</sup>, Beate M. Kümmerer<sup>3</sup>, Athena Labeau<sup>1</sup>, Alexis Brugier<sup>1</sup>, Etienne Simon-Loriere<sup>4</sup>, Julien Burlaud-Gaillard<sup>5</sup>, Cécile Doyen<sup>6</sup>, Laura Pezzi<sup>7</sup>, Thibaud Goupil<sup>2</sup>, Sophia Rafasse<sup>2</sup>, Pierre-Olivier Vidalain<sup>8</sup>, Anne Bertrand Legout<sup>9</sup>, Lucie Gueneau<sup>9</sup>, Raul Juntas-Morales<sup>10</sup>, Rabah Ben Yaou<sup>9</sup>, Gisèle Bonne<sup>9</sup>, Xavier de Lamballerie<sup>7</sup>, Monsef Benkirane<sup>6</sup>, Philippe Roingard<sup>5</sup>, Constance Delaugerre<sup>1,11</sup>, Marc Lecuit<sup>2,12</sup> and Ali Amara<sup>1#\*</sup>

<sup>1</sup> Cell Biology of Virus Infection Team, INSERM U944, CNRS UMR 7212, Institut de Recherche Saint-Louis, Université de Paris, Hôpital Saint-Louis, 75010 Paris, France

<sup>2</sup> Biology of Infection Unit, Institut Pasteur, Inserm U1117, Paris, France

<sup>3</sup> Institute of Virology, University of Bonn Medical Centre, Bonn, Germany

<sup>4</sup> G5 Evolutionary Genomics of RNA Viruses, Institut Pasteur, 28 rue du Dr Roux, 75724 Paris, France

<sup>5</sup> INSERM U1259 MAVIVH et Plateforme IBISA de Microscopie Electronique, Université de Tours, France

<sup>6</sup> Institut de Génétique Humaine, Laboratoire de Virologie Moléculaire, CNRS-Université de Montpellier, 34000 Montpellier, France

<sup>7</sup> Unité des Virus Émergents, Aix-Marseille Univ–IRD190–Inserm 1207 EFS-IRBA, 13005 Marseille cedex 05, France

<sup>8</sup> Equipe Chimie & Biologie, Modélisation et Immunologie pour la Thérapie, Université Paris Descartes, CNRS UMR 8601, Paris, France

<sup>9</sup> Sorbonne Université, INSERM UMRS974, Center of Research in Myology, F-75013 Paris, France.

<sup>10</sup> Département de Neurologie, Centre Hospitalier Universitaire de Montpellier, Montpellier, France.

<sup>11</sup> Laboratoire de Virologie et Département des Maladies Infectieuses, Hôpital Saint-Louis, APHP, 75010 Paris, France

<sup>12</sup> Université de Paris, Department of Infectious Diseases and Tropical Medicine, Necker-Enfants Malades University Hospital, APHP, Institut Imagine, Paris, France

# Contributed equally to the work

\* Corresponding authors: ali.amara@inserm.fr; laurent.meertens@inserm.fr

## ABSTRACT

Chikungunya virus (CHIKV) is a re-emerging Old World alphavirus transmitted to humans by mosquito bites which causes musculoskeletal and joint pain<sup>1-3</sup>. Despite intensive investigations, the identity of the human cellular factors critical for CHIKV infection remains elusive, hampering both the understanding of viral pathogenesis and the development of anti-CHIKV therapies. Here, we identified the Four-and-a-Half LIM domain protein 1 (FHL1)<sup>4</sup> as a host factor required for CHIKV permissiveness and pathogenesis. Ablation of FHL1 expression results in massive inhibition of infection by several CHIKV strains and O'nyong-nyong virus, but not by other alphaviruses or flaviviruses. Conversely, expression of FHL1 enhances infection of cells that do not express it and are poorly susceptible to CHIKV. We show that FHL1 directly interacts with the hypervariable domain of CHIKV nsP3 protein and is essential for viral RNA replication. FHL1 is highly expressed in CHIKV target cells and particularly abundant in muscles<sup>4,5</sup>. Significantly, dermal fibroblasts and muscle cells derived from Emery-Dreifuss muscular dystrophy (EDMD) patients which lack functional FHL1<sup>6</sup> are resistant to CHIKV infection. Importantly, CHIKV infection is undetectable in mice knocked out for the FHL1 gene. Overall, this study shows that FHL1 is a key host dependency factor for CHIKV infection and identifies nsP3-FHL1 interaction as a promising target for the development of anti-CHIKV therapies.

## MAIN TEXT

Several host factors implicated in CHIKV infection have been identified, however none of them accounts for CHIKV tropism for joint and muscle tissues<sup>7-10</sup>. To identify key host factors dictating CHIKV cell permissiveness, we performed a genome-wide CRISPR-Cas9 screen in the HAP1 haploid cell line (Fig.1a, Extended Data Fig. 1). HAP1 cells expressing the human GeCKO v2 single guide RNA libraries A and B, which contains each 3 unique sgRNAs targeting 19,050 genes<sup>11</sup>, were inoculated with CHIKV21, a strain isolated from a patient infected during the 2005-2006 CHIKV outbreak in La Reunion Island<sup>12</sup>. Genomic DNA from lentivirus-transduced cells that survived to CHIKV infection was isolated, amplified and the corresponding integrated sgRNA sequenced. Gene enrichment was assessed using the MAGeCK software<sup>13</sup> (Fig.1a, Extended Data Fig. 1, supplementary Table 1). The top hit of our screen was the gene encoding the Four-and-a-Half LIM protein 1 (FHL1) (Fig.1a, Extended Data Fig. 2a-c), the founding member of the FHL protein family<sup>14</sup>. FHL1 is characterized by the presence of four and a half highly conserved LIM domains with two zinc fingers arranged in tandem<sup>14</sup>. FHL1 is strongly expressed in skeletal muscles and heart<sup>4,14</sup>. In human, there are three FHL1 splice variants: FHL1A, FHL1B and FHL1C<sup>4,15,16</sup>. FHL1A is the most abundantly expressed, primarily detected in striated muscles<sup>4</sup> and fibroblasts<sup>17</sup>. The two other variants FHL1B and C are expressed in muscles, brain and testis<sup>15,16</sup>. We functionally validated the requirement of FHL1 in CHIKV21 infection by using two distinct gRNAs targeting all three FHL1 isoforms (Extended Data Fig. 2a). We generated HAP1 and 293T knockout *FHL1* clones ( $\Delta$ FHL1) and confirmed gene editing by sequencing and western blot analysis (Extended Data Fig. 2d, e, f). FHL1 knockout did not alter cell proliferation and viability as determined by CellTiter-Glo assay (Extended Data Fig. 2g). CHIKV infection and release of infectious particles was



91 drastically inhibited in  $\Delta$ FHL1 cells (Fig.1b, Extended Data Fig. 3a-d). Trans-  
92 complementation of  $\Delta$ FHL1 cells with a human cDNA encoding FHL1A, but not FHL1B  
93 or C, restored both susceptibility to CHIKV21 infection and virus release (Fig. 1c,  
94 Extended Data Fig. 4a-b), indicating that FHL1A is a critical factor for CHIKV21  
95 infection. Expression of FHL2, a member of the FHL family predominantly expressed  
96 in heart<sup>18</sup>, restored CHIKV infection in  $\Delta$ FHL1 cells, albeit to a lower efficiency than  
97 FHL1 (Extended Data Fig. 4c). We then assessed FHL1 dependency of CHIKV strains  
98 from distinct genotypes. FHL1 is important for infection by strains belonging to the  
99 Asian (strain St Martin H20235 2013), the ECSA (East, Central, and South African)  
100 strains Ross and Brazza (MRS1 2011) and the Indian Ocean (IOL) (strain M-899)  
101 lineages (Fig. 1d). Of note, the requirement for FHL1 was less pronounced with CHIKV  
102 37997, a strain from the West African genotype (Fig. 1d). We next tested the  
103 requirement of FHL1 for infection by other alphaviruses. Interestingly, O'nyong-nyong  
104 virus (ONNV), an Old World alphavirus that is phylogenetically very close to CHIKV<sup>1</sup>,  
105 showed a dramatically reduced infection level in  $\Delta$ FHL1 cells (Fig.1e, Extended Data  
106 Fig. 3e). In sharp contrast, other Old World alphaviruses such as Mayaro virus (MAYV),  
107 Sindbis virus (SINV), Semliki Forest Virus (SFV) and Ross River virus (RRV), and New  
108 World encephalitic viruses such as Eastern equine encephalitis virus (EEEV), Western  
109 equine encephalitis virus (WEEV) or Venezuelan equine encephalitis virus (VEEV)  
110 infected HAP1 cells in a FHL1-independent manner (Fig. 1e, f, Extended Data Fig. 3e).  
111 No effect of FHL1 was observed for infection by Dengue virus (DENV) or Zika virus  
112 (ZIKV), two members of the *Flavivirus* genus (Fig. 1g, Extended Data Fig. 3f).  
113 Consistent with the requirement of FHL1 for CHIKV infection, BeWo or HepG2 cells  
114 which are poorly susceptible to CHIKV infection<sup>20,21</sup> and do not express endogenous  
115 FHL1 (Extended Data Fig. 5a) became permissive to the virus upon FHL1A expression

(Fig.1h, Extended Data Fig. 5b-d). This highlights the major role played by FHL1A in human cell permissiveness to CHIKV.

To determine which step in CHIKV life cycle requires FHL1, we challenged parental and  $\Delta$ FHL1 cells with CHIKV particles and quantified the viral RNA at different time points (Fig. 2a). We did not observe any major difference in CHIKV RNA levels in FHL1-deficient cells compared to WT cells at 2h post-infection (Fig. 2a). In contrast, a massive reduction of CHIKV RNA was observed in  $\Delta$ FHL1 cells as early as 6h post-infection (Fig. 2a) which was even greater 24h post-infection, suggesting that FHL1 expression is involved in an early post-entry step of the CHIKV life cycle. We therefore bypassed virus entry and uncoating by transfecting CHIKV RNA into controls or  $\Delta$ FHL1 cells in the presence of  $\text{NH}_4\text{Cl}$  to inhibit further rounds of infection<sup>9</sup>. Upon CHIKV RNA transfection, viral replication was drastically impaired in  $\Delta$ FHL1 cells compared to WT cells (Fig. 2b, Extended Data Fig 6a). To evaluate the contribution of FHL1 in incoming genome translation versus RNA replication, we generated a replication-deficient CHIKV molecular clone (with the GDD motif of the viral polymerase nsP4 mutated to GAA) encoding a *Renilla* luciferase (Rluc) fused to the nsP3 protein as described <sup>22</sup>. Transfection of CHIKV GAA RNA in  $\Delta$ FHL1 or control cells resulted in a similar Rluc activity (Fig. 2c), indicating that FHL1 is dispensable for CHIKV incoming RNA translation. When similar experiments were performed with the WT CHIKV RNA, a massive increase in Rluc activity was observed in control cells but not  $\Delta$ FHL1 24 hpi (Fig. 2d), demonstrating that FHL1 is essential for viral RNA replication. Furthermore, qRT-PCR experiments showed that ablation of FHL1 resulted in a severely reduced synthesis of CHIKV negative strand RNA (Fig. 2e). We then investigated the impact of FHL1 in the production of dsRNA intermediates which are a marker of viral replication complex (vRC) assembly<sup>23</sup>. At 6h post-infection, a massive reduction of dsRNA-

containing complexes was observed in  $\Delta$ FHL1 cells stained with anti-dsRNA mAb when compared to parental cells (Fig. 2f). Consistent with this observation, transmission electron microscopy showed that the formation of plasma membrane-associated spherules and cytoplasmic vacuolar membrane structures, which are alphavirus-induced platforms required for viral RNA synthesis<sup>24</sup>, are absent in  $\Delta$ FHL1 cells (Fig 2g). Altogether, these data show that FHL1 is critical for CHIKV RNA replication and vRC formation in infected cells.

We next investigated FHL1 location during infection. Confocal microscopy studies showed that FHL1 displays a diffuse cytoplasmic distribution in uninfected human fibroblasts. In cells infected for 6h, FHL1-containing foci appeared and colocalized with nsP3 (Extended Data Fig. 6b), a CHIKV non-structural protein orchestrating viral replication in the cytoplasm<sup>25,26</sup>. Indeed, CHIKV nsP3 contains a large C-terminal hypervariable domain (HVD)<sup>25</sup> known to mediate assembly of protein complexes and regulate RNA amplification<sup>25,26</sup>. Interestingly, FHL1 and FHL2 have been reported as putative nsP3 HVD binding partners in mass spectrometry analyses<sup>26,27</sup>. We experimentally validated FHL1-nsP3 interaction (Fig. 2h,i; Extended Data Fig. 6c-g) and found that endogenous FHL1 co-immunoprecipitates with nsP3 from CHIKV-infected cells (Fig. 2h). Consistent with infection studies, both FHL1A and FHL2 co-precipitated with CHIKV nsP3 (Extended Data Fig. 6d). FHL1A-nsP3 interaction is specific for CHIKV as it was not observed with other alphaviruses such as SINV or SFV, which do not depend on FHL1 for infection (Extended Data Fig. 6e). Of note, in  $\Delta$ FHL1 cells, nsP3 retained its ability to bind G3BP1 and 2, two components of the stress granules implicated in CHIKV replication<sup>22,26</sup> (Extended Data Fig. 6e). We next generated chimeric proteins where the HVD region of CHIKV nsP3 is swapped with the corresponding domain of SINV nsP3 and vice versa. Whereas CHIKV-SINV(HVD)

chimeric protein lost its ability to bind FHL1, the HVD of CHIKV in the context of SINV nsP3 protein conferred binding to FHL1 (Extended Data Fig. 6f). Pull-down experiments with purified proteins showed that FHL1A directly binds to WT nsP3 but not to the HVD-deficient variant (Fig. 2i, Extended Data Fig. 6g). We then mapped the binding region within CHIKV nsP3HVD responsible for FHL1A interaction (Fig. 2j, Extended Data Fig. 7). The FHL1 binding domain, referred as HVD-R4, is found in all CHIKV and ONNV strains and is located upstream of the short repeating peptide corresponding to G3BP1/2 binding sites<sup>26</sup> (Fig. 2j, Extended Data Fig. 7a). Deletion of the HVD-R4 region strongly impaired FHL1 interaction with nsP3, without affecting G3BP1/2 binding to the viral protein (Fig. 2j, Extended Data Fig. 7b). To investigate whether FHL1 interaction with the HVD region of nsP3 is required for FHL1 proviral role, we generated two chimeric FHL1A protein either fused to the HVD-R4 peptide (FHL1A-R4) or to a randomized peptide sequence of HVD-R4 (FHL1A-R4\*) as a positive control (Fig. 2k, Extended Data Fig. 7c) and assessed their ability to interact with nsP3. Whereas FHL1A-R4 failed to bind nsP3 (Fig. 2k), FHL1A-R4\* interacted with nsP3 as efficiently as WT FHL1A protein (Fig. 2k). These results indicate that the fused HVD-R4 peptide likely hides the binding site of FHL1A to nsP3, inhibiting their interaction. Furthermore, trans-complementation of  $\Delta$ FHL1 cells with a cDNA encoding FHL1A-R4 did not restore CHIKV21 infection when compared to FHL1A-R4\* or WT FHL1A (Fig. 2l). Consistent with this, *in vitro* transcribed RNA from CHIKV molecular clone mutated in FHL1 binding site ( $\Delta$ R4 or R4\*) showed a strong defect in replication after transfection in 293T cells (Extended Data Fig. 7d). Together these data strongly suggest that the interaction between the HVD region of nsP3 with FHL1 is critical for FHL1 proviral function.

Mutations in the *FHL1* gene have been associated with X-linked myopathies<sup>5,28</sup>, including the Emery–Dreifuss muscular dystrophy (EDMD)<sup>6</sup>, a rare genetic disease characterized by early joint contractures, muscular wasting and adult-onset cardiac disease<sup>29</sup>. We studied the permissiveness to CHIKV of dermal fibroblasts and myoblasts from four EDMD male patients carrying *FHL1* gene mutations as well as from two healthy donors (Extended Data Fig.8a). A detailed clinical description of P1, P2 and P3 has been reported<sup>6</sup>, and patient P4 presented with EDMD and additional clinical abnormalities (see methods). Analysis of P4 *FHL1* gene revealed the insertion of a full-length LINE-1 retrotransposon sequence in exon 4 (Extended Data Fig.8b). *FHL1* expression is severely reduced in primary cells from all four EDMD patients as established by immunoblot analysis (Fig. 3a). Infection studies showed that fibroblasts and myoblasts from those EDMD patients are resistant to CHIKV21 and M-899 Mauritian strains (Fig. 3b-d, Extended Data Fig.8c), and exhibit a massive defect in the release of infectious particles (Fig. 3d), in contrast to healthy donor cells. Similar results were obtained with the CHIKV strains Brazza, Ross and H20235 (Fig. 3e, Extended Data Fig.8d). *FHL1*-null myoblasts and fibroblasts remained highly susceptible to MAYV, which does not rely on *FHL1* for replication (Fig. 3e). Trans-complementation of EDMD fibroblasts by a lentivirus encoding WT *FHL1A* restored CHIKV viral antigen synthesis (Fig. 3f, Extended Data Fig.8e) and infectious particle release (Fig. 3g).

To directly assess the role of *FHL1* in chikungunya pathogenesis, we conducted *in vivo* experiments in mice expressing or not *FHL1*. Human and mouse *FHL1* orthologues are highly conserved (Extended Data Fig.9a). Murine *FHL1* interacts with CHIKV nsP3 and enhances viral infection, albeit less efficiently than its human orthologue (Extended Data Fig.9 b-d). Moreover, CHIKV infection was strongly impaired in the murine muscle cell C2C12 deleted for the *fh1* gene (Extended Data

Fig.9 e-f). Susceptibility to CHIKV infection of young mice deficient or not for FHL1 was then tested. CHIKV actively replicated in tissues of WT littermates, as previously reported<sup>20</sup>, but virtually no infectious particles were detected in tissues of FHL1-null mice (Fig. 4a). Moreover, necrotizing myositis with massive infiltrates and necrosis of the muscle fibers were observed in skeletal muscle of WT littermates, while FHL-null mouse muscle showed no detectable pathology (Fig. 4b). Immunolabelling with Ab against CHIKV E2 protein, FHL1 and vimentin in muscle revealed that in young WT mice, CHIKV mainly targets muscle fiber expressing FHL1, whereas muscle cells of FHL1-null mice show no label for CHIKV nor for FHL1 (Fig. 4c). These experiments demonstrate that *FHL1* knock out mice are resistant to CHIKV infection.

In summary, this study shows that FHL1 is a critical CHIKV host dependency factor for infection and pathogenesis. *In vivo*, FHL1 expression pattern, which accounts for the clinical presentation of EDMD, also reflects CHIKV tissue tropism for skeletal muscles and joints. This suggests that the hijacking of FHL1 by CHIKV during infection may, on top of allowing viral replication, lead to cellular dysfunctions contributing to muscular and joint pains that are the hallmark of chikungunya disease<sup>1,2</sup>. Mechanistically, FHL1 interacts with the HVD domain of nsP3 to enable viral RNA synthesis and viral replication complex formation. The alphavirus nsP3 HVD domain is an intrinsically disordered region that binds distinct sets of cellular proteins<sup>23,26,30</sup> such as the G3BP1 and G3PB2, two key components and markers of stress granules that are important for the replication of CHIKV and other alphaviruses<sup>22,26</sup>. G3BP1/2 nsP3 interactions are thought drive a common alphavirus-specific mechanism that is important for assembly of the replication complex and stabilization of viral G RNA<sup>22,23,26</sup>. FHL1 interacts with a nsP3 HVD region which is located away from G3BP1/2 binding sites. Therefore, FHL1 and G3BP proteins likely play distinct roles

during CHIKV replication. In contrast to G3BPs, FHL1 is selectively used by CHIKV, suggesting that it may accomplish a specific and essential function in CHIKV RNA amplification. Upon interaction with FHL1, CHIKV nsP3 HVD may adopt a unique conformation that is critical for the initiation of viral replication. Interestingly, intrinsically disordered domains (IDD) such as the nsP3 HVD have also been shown to induce liquid-liquid phase separations<sup>31</sup> and negative-stranded RNA viruses use proteins displaying IDDs to form liquid organelles for their replication<sup>32</sup>. Indeed, in CHIK-infected cells, nsP3 forms intracellular granules reminiscent of these virus-induced inclusions<sup>33,34</sup>. FHL1 may regulate the formation and/or the dynamic of such granules to create an optimal environment for efficient CHIKV RNA amplification. FHL1 contains four LIM domains arranged in tandem known to function as a modular protein binding interface regulating diverse cellular pathways<sup>35</sup>. FHL1 has been shown to scaffold MAPK components (Raf-1/MEK2/ERK2) to the stretch sensor Titin N2B to transmit MAPK signals that regulate muscle compliance and cardiac hypertrophy<sup>36,37</sup>. One may speculate that, during CHIKV infection, FHL1 may be hijacked from its physiological function in sarcomere extensibility and intracellular signaling to act as scaffolding protein promoting CHIKV RNA amplification.

In conclusion, this study provides major insights into the understanding of CHIKV interactions with its target host cell. Although other host-factors have been identified as required for CHIKV infection, none of them fully account for the specific joint and muscular pathology which is the hallmark of CHIKV and gave its name to its associated disease, chikungunya, which means “that which bends up” in Makonde, to describe the posture of patient with muscle and joint pain. The hijacking of FHL1 by nsP3 during CHIKV infection is unique and constitutes a critical clue that paves the way to fully decipher the pathogenesis of chikungunya disease. Targeting FHL1A–

265 nsP3 interactions now stands as an attractive therapeutic approach to combat CHIKV  
266 pathogenesis.  
267



## METHODS

**Cell culture.** HAP1 cells (Horizon Discovery), which are derived from near-haploid chronic myeloid leukemia KBM7 cells, were cultured in IMDM supplemented with 10% FBS, 1% penicillin-streptomycin (P/S) and GlutaMAX (Thermo Fisher Scientific). 293FT (Thermo Fisher Scientific), HEK-293T (ATCC), Vero E6 (ATCC), HepG2 (kind gift of Olivier Schwartz, Institut Pasteur, Paris, France), primary myoblasts and primary fibroblasts were cultured in DMEM supplemented with 10% FBS, 1% penicillin-streptomycin, 1% GlutaMAX and 25 mM Hepes. Human placenta choriocarcinoma Bewo cells were cultured in DMEM supplemented with 5% FBS, 1% penicillin-streptomycin, 1% GlutaMAX and 25 mM Hepes. AP61 mosquito (*Aedes pseudoscutellaris*) cells (gift from Philippe Despres, Institut Pasteur, Paris, France) were cultured at 28°C in Leibovitz medium supplemented with 10% FCS, 1% P/S, 1% glutamine, 1X non-essential amino acid, 1X Tryptose phosphate and 10 mM Hepes. All cell lines were cultured at 37°C in presence of 5% CO<sub>2</sub> with the exception of AP61 that were maintained at 28°C with no CO<sub>2</sub>.

**Virus strains and culture.** CHIKV21 (strain 06-21), ZIKV (HD78788) (both are kind gift from Philippe Despres, Institut Pasteur, Paris, France), CHIKV West Africa (strain 37997, accession nb AY726732.1) and dengue virus serotype 2 DENV (16681) viruses were propagated in mosquito AP61 cell monolayers with limited cell passages. CHIKV-Brazza-MRS1 2011, CHIKV-Ross, CHIKV-St Martin H20235 2013-Asian, RRV (strain 528v), MAYV (strain TC 625), ONNV (strain Dakar 234), SINV (strain Egypt 339), EEEV (strain H178/99), VEEV (strain TV83 vaccine), WEEV (strain 47A), SFV (strain 1745) were obtained from the European Virus Archive (EVA) collection and propagated with limited passage on Vero E6 cells.

pCHIKV-M-Gluc (see plasmid sections) and pCHIKV-mCherry molecular clones were derivate of pCHIKV-M constructed from a CHIKV (strain BNI-CHIKV\_899) isolated from a patient during Mauritius outbreak in 2006. To generate infectious virus from CHIKV molecular clones, capped viral RNAs were generated from the NotI-linearized CHIKV plasmids using a mMESSAGE mMACHINE SP6 or T7 Transcription Kit (Thermo Fischer Scientific) according to manufacturer's instructions. Resulting RNAs were purified by phenol:chloroform extraction and isopropanol precipitation, resuspended in water, aliquoted and stored at -80°C until use. Thirty µg of purified RNAs were transfected in BHK21 with lipofectamine 3000 reagent and supernatants harvested 72 hours later were used for viral propagation on Vero E6 cells. For all the viral stock used in flow cytometry analysis experiments, viruses were purified through a 20% sucrose cushion by ultracentrifugation at 80,000xg for 2 hours at 4°C. Pellets were resuspended in HNE1X pH7.4 (Hepes 5 mM, NaCl 150 mM, EDTA 0.1 mM), aliquoted and stored at -80°C. Viral stock titers were determined on Vero E6 cell by plaque assay and are expressed as PFU per ml. Virus stocks were also determined by flow cytometry as previously described<sup>38,39</sup> Briefly, Vero E6 cells were incubated for 1h with 100µl of 10-fold serial dilutions of viral stocks. The inoculum was then replaced with 500µl of culture medium and the percent of E2 expressing cells was quantified by flow cytometry at 8 hpi. Virus titers were calculated using the following formula and expressed as FACS Infectious Units (FIU) per ml. [Titer (FIU/ml) = (average % of infection) x (number of cells in well) x (dilution factor) / (ml of inoculum added to cells)].

**Reagents.** . The following antibodies were used: anti-FHL1 mAb (ref MAB5938, R & D Systems), anti-FHL1 rabbit Ab (ref NBP1-88745, Novus Biologicals), anti-vimentin

318 antibody (ab24525, abcam), anti-GAPDH mAb (ref SC-47724, Santa Cruz  
319 Biotechnology), polyclonal rabbit anti-HA (ref 3724, Cell Signaling Technology), anti-  
320 FLAG M2 mAb (ref F1804, SIGMA), anti-RFP (ref 6G6, Chromotek), anti-CHIKV E2  
321 mAb (3E4 and 3E4 conjugated-CY3), anti-alphavirus E2 mAb (CHIK-265 was a kind  
322 gift from Michael Diamonds, University school of medicine, St Louis, USA), anti-EEEV  
323 E1 mAb (ref MAB8754, Sigma), anti-pan-flavivirus E protein mAb (4G2), anti-dsRNA  
324 J2 mAb (Scicons), Alexa Fluor™ 488-conjugated goat anti-rabbit IgG (A11034,  
325 Invitrogen), Alexa Fluor™-647-conjugated goat anti-chicken IgG (ab150175, abcam),  
326 Alexa Fluor™ 488-conjugated goat anti-mouse IgG (115-545-003, Jackson  
327 ImmunoResearch), Alexa Fluor™ 647-conjugated goat anti-mouse IgG (115-606-062,  
328 Jackson ImmunoResearch), peroxidase-conjugated donkey anti-rabbit IgG (711-035-  
329 152, Jackson ImmunoResearch), and anti-mouse/HRP (P0260, Dako Cytomotion).  
330 FLAG magnetic beads (ref M8823, SIGMA), HA-magnetic beads (ref 88837, Thermo  
331 Fisher Scientific) and anti-RFP coupled to magnetic agarose beads (RFP-Trap MA,  
332 Chromotek) were used for immunoprecipitation experiments.

333

334 **CRISPR genetic screen.** The GeCKO v2 human CRISPR pooled libraries (A and B)  
335 encompassing 123,411 different sgRNA targeting 19,050 genes (cloned in the  
336 plentiCRISPR v2) were purchased from GenScript. Lentiviral production was prepared  
337 independently for each half-library in 293FT cells by co-transfecting sgRNA plasmids  
338 with psPAX2 (Kind gift from Nicolas Manel, Institut Curie, Paris, France) and pCMV-  
339 VSV-G at a ratio of 4:3:1 with lipofectamine 3000 (Thermo Fisher Scientific).  
340 Supernatants were harvested 48h after transfection, cleared by centrifugation (750 x  
341 g for 10 min), filtered using a 0.45 µm filter and purified through a 20% sucrose cushion  
342 by ultracentrifugation (80,000 x g for 2 hours at 4°C). Pellets were resuspended in

HNE1X pH7.4, aliquoted and stored at -80°C. HAP1 cells were transduced by spinoculation (750 x g for 2 hours at 32°C) with each CRISPR-sgRNA lentiviral libraries at a multiplicity of infection (MOI) of 0.3 and a coverage of 500 times the sgRNA representation. Cells were selected with puromycin for 8 days and expanded. Sixty million cells from each library were pooled and infected with CHIKV21 using a MOI of 1. Simultaneously forty million of non-infected pooled cells were pelleted and kept at -80°C to serve as a reference of the library representation at time of infection. Approximately 5 days after infection, cytopathic effect was detectable and surviving cells were collected 2 weeks later. Genomic DNA was extracted from selected cells or non-infected pooled cells using QIAamp DNA column (Qiagen), and inserted gRNA sequences were amplified and subject to next generation sequencing on an Illumina MiSeq (Plateforme MGX, Institut Génomique Fonctionnelle, Montpellier, France). gRNA sequences were analyzed using the MAGeCK software<sup>13</sup>. Additionally, gRNA sequences were analyzed using the RIGER software following previously published recommendation<sup>40</sup>.

**FHL1 editing.** FHL1 was validated using two independent sgRNA targeting the exon 3 and exon 4, which are common to all FHL1 isoforms. sgRNA1, 5'-GAGGACTCCCCCAAGTGCAA-3' and sgRNA2, 5'-GCAGTCAAACCTTCTCCGCCA-3' were cloned into the plasmid lentiCRISPR v2 according to Zhang lab's recommendation. HAP1 and 293FT cells were transiently transfected with the plasmid expressing individual sgRNA and selected with puromycin until all mock-transfected cells died (approximately 72 hours). Transfected cells were used to ascertain gRNA-driven resistance to CHIKV cytopathic effect, and clonal cell lines were isolated by limiting dilution and assessed by immunoblot for FHL1 expression.

368

369 **Infection assay.** For infection quantification by flow cytometry analysis, cells were  
370 plated in 24-well plates. Cells were infected for 24 (293T) or 48 hours (HAP1),  
371 trypsinized and fixed with 2% (v/v) paraformaldehyde (PFA) diluted in PBS for 15 min  
372 at room temperature. Cells were incubated for 30 min at 4°C with 1µg/ml of either the  
373 3E4 anti-E2 mAb for CHIKV strains and ONNV) or the CHIKV 265 anti-E2 mAb for  
374 MAYV or the anti-E1 mAb for EEEV or anti-pan-flavivirus E 4G2 for DENV and ZIKV.  
375 Ab were diluted in permeabilization flow cytometry buffer (PBS supplemented with 5%  
376 FBS, 0.5% (w/v) saponin, 0.1% Sodium azide). After washing, cells were incubated  
377 with 1µg/ml of Alexa Fluor 488 or 647-conjugated goat anti-mouse IgG diluted in  
378 permeabilization flow cytometry buffer for 30 min at 4°C. Acquisition was performed on  
379 an Attune NxT Flow Cytometer (Thermo Fisher Scientific) and analysis was done by  
380 using FlowJo software (Tree Star). To assess infectious viral particles release during  
381 infection, cells were inoculated for 3 hours with viruses, washed once and then  
382 maintained in culture medium over a 72-hour period. At indicated time points  
383 supernatants were collected and kept at -80°C. Vero E6 cells were incubated with 10-  
384 fold serial dilution of supernatant for 24 hours and E2 expression was quantified by  
385 flow cytometry as described above.

386 For detection of infected cells by immunofluorescence, control and  $\Delta$ FHL1 HAP1 cells  
387 were plated on Lab-Tek II CC2 glass slide 8 wells (Nunc). Cells were inoculated with  
388 CHIKV21 strain (MOI of 20) or CHIKV-nsP3-mCherry (MOI of 20) for 48 hours, then  
389 washed thrice with cold PBS and fixed with 4% (v/v) PFA diluted in PBS for 20 min at  
390 room temperature. CHIKV E2 protein was stained with the 3E4 mAb at 5 µg/ml,  
391 followed by a secondary staining with 1µg/ml of Alexa 488-conjugated goat anti-mouse  
392 IgG. Both antibodies were diluted in PBS supplemented with 3% (w/v) BSA and 0.1%

393 saponin. Slides were mounted with ProLong Gold antifade reagent containing 4,6-  
 394 diamidino-2-phenylindole (DAPI) for nuclei staining (Thermo Fisher Scientific).  
 395 For colocalization experiments, cells infected with CHIKV-nsP3-mCherry (MOI of 20)  
 396 were stained with 10 µg/ml of the anti-FHL1 mAb, followed by a secondary staining  
 397 with 1µg/ml of Alexa 488-conjugated goat anti-mouse IgG.  
 398 For detection of dsRNA foci, control and  $\Delta$ FHL1 293T cells were plated on Lab-Tek II  
 399 CC2 glass slide 8 wells (Nunc) and infected with CHIKV21 strain (MOI of 50) for 4 or  
 400 6 hours. After fixation with 4% (v/v) PFA diluted in PBS, cells were stained with 5 µg/ml  
 401 of the anti-dsRNA mAb, followed by a secondary staining with 1µg/ml of Alexa 488-  
 402 conjugated goat anti-mouse IgG. Both antibodies were diluted in PBS supplemented  
 403 with 3% (w/v) BSA and 0.1% Triton 100X. Of note, no dsRNA foci were detectable at  
 404 4hpi.  
 405 Fluorescence microscopy images were acquired using a LSM 800 confocal  
 406 microscope (Zeiss).  
 407  
 408 **Plasmid constructions.** To generate the C-terminal HA-tagged FHL1 isoforms, the  
 409 cDNAs of FHL1A (NM\_001449.4), FHL1B (XM\_006724746.2) and FHL1C  
 410 (NM\_001159703.1) were purchased from Genscript. Coding sequence (CDS) were  
 411 amplified with a common FHL1 Fwd primer 5'-  
 412 CCGGAGAATTGCGCGCCATGGCGGAGAAGTTTGACTGCCACTACTGC-3'; and  
 413 specific FHL1A Rev primer 5'-AATAGTTTAG**GCGGCCGCT**CAAGCGTAATCTGGAA  
 414 CATCGTATGGGTATCCTCCAGCGGCCGACCAGCTTTTTTGGCACAGTCGGGACAA  
 415 TACACTTGCTCC-3'; or FHL1B and C specific Rev primer 5'-  
 416 AATAGTTTAG**GCGGCCGCT**CAAGCGTAATCTGGAACATCGTATGGGTATCCTCCA  
 417 GCGGCCGACGCGGAGCATTTTTTGCAGTGGAAGCAGTAGTCGTGCC-3' (underline,

segment hybridizing with the target sequence; bold, restriction endonuclease site for cloning); and cloned into pLVX-IRES-ZsGreen1 vector (Takara). Using the same approach, coding sequence of murine FHL1 (NM\_001077362.2) was amplified with a mFHL1 Fwd primer 5'-CCGGAGAATTGCGCCG**CCATGGCTTCTCAAAGACACTCAG**  
**GTCCCTCC**-3' and mFHL1 Rev primer 5'-AATAGTTTAGCGGCCGCTCAAGCGTAA  
TCTGGAACATCGTATGGGTATCCTCCAGCGGCCG**ACAGCTTTTTGGCACAGTCA**  
**GGGCAATACACCGCTC**-3', and cloned into pLVX-IRES-ZsGreen1 vector. C-terminal HA-tagged FHL2 coding sequence was synthesized by Genscript and subcloned into pLVX-IRES-ZsGreen1 vector. The plasmids pCI-neo-3×FLAG plasmids expressing the CHIKV nsP3 and nsP4, the Sindbis virus (SINV) and Semliki Forest virus (SFV) nsP3 proteins were previously described<sup>41</sup>. The CHIKV nsP3  $\Delta$ HVD,  $\Delta$ R1 to  $\Delta$ R4 were generated by site-directed mutagenesis (QuickChange XL Site-Directed Mutagenesis Kit, Agilent) using the following sets of primers:  $\Delta$ HVD-Fwd (5'-CGTAAGTCCAAGGGAATATTGATGATCTTCCCAGGAGTCTGC-3') and  $\Delta$ HVD-Rev (5'-GCAGACTCCTGGGAAGATCATCAATATTCCCTTGGACTTACG-3');  $\Delta$ R1-F: (5'-GTACCTGTGCGCGCCGCCCAGAGAGCTGTGTCCGGTCGTACAAGA  
AAC-3') and  $\Delta$ R1-R: (5'-GTTTCTTGTACGACCGGACACAGCTCTCTGGGCGGCG  
CGACAGGTAC-3');  $\Delta$ R2-F: (5'-GAAACAGCGGAGACGCGTGACAGTACCGCCA  
CGGAACCGAATC-3') and  $\Delta$ R2-R: (5'-GATTCGGTTCGGTGGCGGTACTGTCACGC  
GTCTCCGCTGTTTC-3');  $\Delta$ R3-F: (5'-CTTCTTACCAGGAGAAGTGTGATGACTTGA  
CAGACAGC-3') and  $\Delta$ R3-R: (5'-GCTGTCTGTCAAGTCATCACACTTCTCCTGGTAA  
GAAG-3');  $\Delta$ R4-F (5'-GACGAGAGAGAAGGGAATATAACACCGAGTACCGCCACG  
GAACCGAATC-3') and  $\Delta$ R4-R (5'-GATTCGGTTCGGTGGCGGTACTCGGTGTTATA  
TTCCCTTCTCTCTCGTC-3').

442 The plasmids expressing the chimeric nsP3 CHIKV-HVD SINV and nsP3 SINV-HVD  
 443 CHIKV were obtained as follows. First, the DNA sequence coding for the N-terminal  
 444 parts of the CHIKV or SINV nsP3 (MD-AUD region) are obtained by PCR using the  
 445 pCI-neo-3×FLAG expression plasmids as templates and the following sets of primers:  
 446 3xFLAG\_NotI-F (5'-ACTGAGCGGCCGCATGGACTACAAAGACCATGAC-3') and  
 447 Overlap-CHIKV-SINV-R (5'-GCTGTTCTGGCACTTCTATATATTCCCTTGGA  
 448 CTTACG-3'), or 3xFLAG\_NotI-F and Overlap-SINV-CHIKV-R (5'-  
 449 CAGACTCCTGGGAAGATCTGTACTTACGGGCGGGAAC-3') for CHIKV and SINV  
 450 constructs, respectively. HVD coding sequences were also generated by PCR using  
 451 the following primers: Overlap-CHIKV-SINV-F (5'-  
 452 CGTAAGTCCAAGGGAATATATAGAAGTGCCAGAACAGC-3') and nsP3-  
 453 SINV\_BamHI-R (5'-ACTGAGGATCCTTAGTATTCAGTCCTCCTGCTC-3') for SINV  
 454 HVD, and Overlap-SINV-CHIKV-F (5'-GTTCCCGCCCGTAAGTACAGATCTTCCCA  
 455 GGAGTCTG-3') and nsP3-CHIKV\_BamHI-R (5'-ACTGAGGATCCTCATAACTCGT  
 456 CGTCCGTG-3') for CHIKV HVD. Next, the CHIKV-HVD-SINV and SINV-HVD-CHIKV  
 457 PCR-fragments were obtained by overlap extension PCR using the previously  
 458 obtained PCR-products and the following sets of primers: 3XFLAG\_NotI-F and nsP3-  
 459 SINV\_BamHI-R or nsP3-CHIKV\_BamHI-R. Finally, the chimeric PCR fragments were  
 460 cloned into a NotI-BamHI digested pLVX-IRES-ZsGreen1 vector (Takara).  
 461 The plasmid expressing FHL1A-R4 and FHL1A-R4\* fusion proteins were obtained by  
 462 overlap extension PCR approach as well. First, the FHL1A part which is common to  
 463 both constructs was amplified from a cDNA template (Genscript, NM\_001449.4) using  
 464 the common FHL1 Fwd primer (5'-  
 465 CCGGAGAATTCGCCGCCATGGCGGAGAAGTTTGACTGCCACTACTGC-3') and  
 466 the Overlap-FHL1A-Fusion Rev primer (5'- CGCCCTGGAAGTACAGGTTCTCGCCG



467 CCGCCCAGCTTTTTGGCACAGTCGGGACAATAC-3'). Second, nsP3-R4 and -R4\*  
 468 portions were obtained by PCR using either the pCI-neo-3×FLAG-nsP3 expression  
 469 plasmid or the pCHIKV-SG45-R4\* plasmid (containing the randomized R4 region) as  
 470 templates and the following set of primers: Overlap-FHL1-fusion-Fwd (5'-  
 471 CGAGAACCTGTACTTCCAGGGCGGCGGCGGCCCCATGGCTAGCGTCCGATTCT  
 472 TTAG-3') and FHL1-fusion-Rev (5'-AATAGTTTAGCGGCCGCTCAAGCGTAATCT  
 473 GGAACATCGTATGGGTAGCCGCCGCCGGTGGTGCCTGAAGAGACATTGCTG-  
 474 3') for R4 construct, or FHL1-fusion-Rand-Rev primer (5'-  
 475 AATAGTTTAGCGGCCGCTCAAGCGTAATCTGGAACATCGTATGGGTAGCCGCC  
 476 GCCCCTCACCTCGGCGCACATGG-3') for the randomized R4\* construct. Next, the  
 477 FHL1A-R4 and FHL1A-R4\* PCR-fragments were obtained by PCR using the  
 478 previously obtained PCR-products and the outer sets of primers: FHL1A Fwd and  
 479 FHL1-fusion-Rev or FHL1-fusion-Rand-Rev. Amplification fragments were cloned into  
 480 a NotI-EcoRI digested pLVX-IRES-ZsGreen1 vector (Takara).  
 481 To obtain pCHIKV-M-Gluc a viral sequence encompassing the CHIKV 26S promoter  
 482 and a part of the capsid protein sequence was amplified from pCHIKV-M using primers  
 483 5'-TATGCGTTTAAACCATGGCCACCTTTGCAAGCTCCAGATC-3' and 5'-  
 484 GCTTCTTATTCTTCCGATTCCTGCGTGG-3', cut with PmeI and BssHII and  
 485 assembled together with an AgeI-PmeI fragment from pCHIKVRepl-Gluc<sup>42</sup> into an  
 486 AgeI-BssHII cut vector. From the resulting plasmid the AgeI-BssHII fragment was  
 487 released and ligated together with a BssHII-SfiI fragment from pCHIKV-M<sup>43</sup> into  
 488 pCHIKV-M cut with AgeI and SfiI.  
 489 To establish pCHKV-Rluc-GAA two PCR fragments were amplified from pCHIKV-WT  
 490 using primers CHIKV 5590 F (5'-AGACTTCTTACCAGGAGAAGTG-3') and Bo422 (5'-  
 491 CGACTCCATGTATTATGTTaccgctgcGATGAAGGCCGCGCACGCGG-3') or Bo421

492 (5'-CCGCGTGCGCGGCCTTCATCgcagcgggtAACATAATACATGGAGTCG-3') and  
 493 CHIKV 8512 R (5'-GAAGTTGTCCTTGGTGCTGC-3'), respectively. The obtained  
 494 fragments were fused via PCR amplification using the outer primers CHIKV 5590 F  
 495 and CHIKV 8512 R. The resulting fragment was cut with AgeI and BglI and inserted  
 496 into pCHIKV-Rluc cut with the same restriction enzymes.  
 497 For generation of CHIKV-Rluc-ΔR4 and CHIKV-Rluc-R4\* first PCR fragments  
 498 encompassing the desired changes were amplified and assembled as follows: 1)  
 499 CHIKV-Rluc-ΔR4: two fragments amplified from CHIKV-Rluc using Bo408 (5'-  
 500 CACCACGTGCTCCTGGTCAGTG-3') and Bo1259 (5'-  
 501 gattcggttccgtggcgggtactcggtgttatattcccttctctctcgta-3') or Bo1258 (5'-  
 502 tgacgagagagaagggaatataacaccgagtaccgccacggaaccgaatc-3') and Bo409 (5'-  
 503 GACTTCCTCCAGGGTGTTCACC-3'), respectively, were fused together using the  
 504 outer primers Bo408 and Bo409. 2) CHIKV-Rluc-R4\*: the randomized sequence  
 505 cassette was obtained sequentially from three successive PCRs: First PCR fragment  
 506 was generated using primers Bo1260 (5'-  
 507 AGCACCGTGCCCCTGCCCCGCCCTGAGGAGGGCCAGCTTCGCCGACACCATGG  
 508 AGCAGACC-3') and Bo1261 (5'-  
 509 CCTCACCTCGGCGCACATGGGGAACTGCTCGGCCACGGTCTGCTCCATGGTGT  
 510 CGGCGAA-3'). Then, it was fused at the 5' end with a PCR fragment amplified from  
 511 CHIKV-Rluc with Bo408 and Bo1262 (5'-  
 512 TCAGGGCGGGCAGGGGCACGGTGCTgttatattcccttctctctcgta-3'). Next, the  
 513 resulting fragment is further fused at the 3' end with a PCR fragment amplified from  
 514 CHIKV-Rluc with Bo1263 (5'-  
 515 GTTCCCCATGTGCGCCGAGGTGAGGccgagtaccgccacggaaccgaatc-3') and Bo409,  
 516 using the outer primers Bo408 and Bo409. Finally, the PCR fragments containing the

$\Delta R4$  and  $R4^*$  mutations were cut with SacII and AgeI and fused in each case with a NgoMIV-SacII fragment derived from CHIKV-Rluc (SG45) and were cloned into a NgoMIV-AgeI digested SG45 plasmid.

**Trans-complementation and over expression experiments.** The lentiviral plasmids containing FHL1 isoforms were packaged as described above (see 'CRISPR genetic screen' section). Cells of interest were stably transduced by spinoculation (750 x g for 2 hours at 32°C) with these lentiviruses and, when necessary, sorted for GFP-positive cells by flow cytometry. For trans-complementation assays cells were inoculated with CHIKV21 for 48 hours. Cells were then collected and processed for E2 expression by flow cytometry. For ectopic expression, cells were plated on 24-well plates ( $5 \times 10^4$ ) and incubated with CHIKV-M-GLuc and CHIKV21, and either processed for E2 expression by flow cytometry or infectious virus yield quantification on Vero E6 cells.

**Kinetic of infection by qPCR assay.** Control and  $\Delta FHL1$  HAP1 cells were plated on 60 mm dishes (400,000 cells) and inoculated with CHIKV21 (MOI of 5). At indicated time point cells were washed thrice with PBS, incubated with trypsin 0.25% for 5 min at 37°C to remove cells surface bound particles, and total RNA was extracted using the RNeasy plus mini kit (Qiagen) according to manufacturer's instruction. cDNAs were generated from 500 ng total RNA by using the Maxima First Strand Synthesis Kit following manufacturer's instruction (Thermo Fisher Scientific). Amplification products were incubated with 1 Unit of RNase H for 20 min at 37 °C, followed by 10 min at 72°C for enzyme inactivation, and diluted 10-fold in DNase/RNase free water. Real time quantitative PCR was performed using a Power Syber green PCR master Mix (Fisher Thermo Scientific) on a Light Cycler 480 (Roche). The primers used for qPCR were:

E1-C21\_F (5'-ACGCAGTTGAGCGAAGCAC-3'), E1-C21\_R (5'-CTGAAGACATTG  
GCCCCAC-3') for viral RNA quantification, and Quantitect primers for GAPDH were  
purchased from Qiagen. The relative expression quantification was performed based  
on the comparative threshold cycle ( $C_T$ ) method, using GAPDH as endogenous  
reference control. CHIKV negative strand RNA was quantified as previously  
described<sup>44</sup>. Briefly, cDNA were generated from 1 µg total RNA using a primer  
containing a 5' tag sequence CHIKV(-)Tag (5'-  
GGCAGTATCGTGAATTCGATGCCGCTGTACCGTCCCCATTCC-3') and the  
SuperScript II reverse transcriptase following the manufacturer's instruction (Thermo  
Fisher Scientific). Amplifications products were diluted 10-fold and used for real time  
quantitative PCR with the following primers CHIKV(-)fwd (5'-  
GGCAGTATCGTGAATTCGATGC-3') and CHIKV(-)rev (5'-ACTGCTGAGTCCAAAG  
TGGG-3'). The 133 bp sequence corresponding to the amplified cDNA was  
synthesized by Genescript and serially diluted (650 to 6.5x10<sup>9</sup> genes copies/µl) to  
generate standard curves.

**Genomic viral RNA transfection and kinetic of viral amplification.** To assess  
CHIKV RNA replication within the cells, we transfected control and ΔFHL1 cells with  
capped genomic viral RNA generated from pCHIKV-M-Gluc (see 'Virus strains and  
culture' section). Cells were plated on 48 well plate (3x10<sup>4</sup> cells) and transfected with  
100 ng of purified RNA using the Lipofectamine MessengerMax reagent according to  
the manufacturer's instruction (Thermo Fisher Science), and cells were cultured in  
absence or presence of 15 mM NH<sub>4</sub>Cl to prevent subsequent viral propagation. At  
specific times, cells were washed once with PBS and lyzed with Gaussia lysis buffer.  
Lysates were kept at -20°C until all samples were collected. Luciferase activity was

measured by using the Pierce Gaussia Luciferase Glow assay kit on a TriStar2 LB 942 with 20 µl of cell lysate, 20 µl of substrate and 2s integration time.

The same experimental approach was used to monitor luciferase activity from capped genomic viral RNA generated from pCHIKV-Rluc WT (SG45), pCHIKV-Rluc-GAA, pCHIKV-Rluc-ΔR4 and pCHIKV-Rluc-R4\* mutants. Luciferase activity was measured using the Renilla Luciferase assay system (Promega) on a TriStar2 LB 942 with 20 µl of cell lysate, 20 µl of substrate and 2.5s integration time.

**Immunoblot.** Cell pellet were lysed in Pierce™ IP Lysis Buffer (Thermo Fisher Scientific) containing Halt™ Protease and Phosphatase Inhibitor Cocktail (Thermo Fischer Scientific) for 30 min at 4°C. Equal amount of protein, determined by DC™ Protein Assay (BioRad), were prepared in LDS Sample Buffer 4X (Pierce™) containing 25 mM dithiothreitol (DTT) and heated at 95°C for 5 min. Samples were separated on Bolt™ 4-12% Bis-Tris gels in Bolt® MOPS SDS Running Buffer (Thermo Scientific), and proteins were transferred onto a PVDF membrane (BioRad) using the Power Blotter system (Thermo Fischer Scientific). Membranes were blocked with PBS containing 0.1% Tween-20 and 5% non-fat dry milk and incubated overnight at 4°C with primary antibody. Staining was revealed with corresponding horseradish peroxidase (HRP)-coupled secondary antibodies and developed using SuperSignal™ West Dura Extended Duration Substrate (Thermo Fisher Scientific) following manufacturer's instructions. The signals were acquired through Fusion Fx camera (VILBERT Lourmat).

**Co-immunoprecipitation assay.** HEK-293T cells were plated in 10 cm dishes ( $5 \cdot 10^6$  cells/ dish). Twenty-four hours later, the cells were transfected with a total of 15 µg of

592 DNA expression plasmids (7.5 µg of each plasmid in co-transfection assays). Twenty-  
 593 four hours post-transfection the cells washed once with PBS and collected with a cell  
 594 scrapper. After 5 min centrifugation (400 x g for 5 min), cells pellets were lysed for 30  
 595 min in cold IP lysis buffer supplemented with Halt™ Protease and Phosphatase  
 596 Inhibitor Cocktail, and then cleared by centrifugation for 15 min at 6,000 x g.  
 597 Supernatants were incubated overnight at 4°C, with either anti-FLAG magnetic beads  
 598 or HA magnetic beads (see 'reagent' section above). Beads were washed three times  
 599 with BO15 buffer (20 mM Tris-HCl pH 7.4, 150 mM NaCl, 5 mM MgCl<sub>2</sub>, 10% Glycerol,  
 600 0.5 mM EDTA, 0.05% Triton, 0.1% Tween-20). The retained complexes were eluted  
 601 twice with either 3xFLAG-peptide (200 µg/ml; SIGMA F4799-4MG) or HA peptide (400  
 602 µg/ml; Roche# 11666975001) for 30 min at room temperature. Samples were prepared  
 603 and subjected to immunoblot as described above. For input, 1% of whole cell lysate  
 604 were loaded on the gel.

605

606 **Bacterial expression, purification and GST pull down assay.** To express nsP3,  
 607 nsP3ΔHVD as glutathione S-transferase fusion proteins, their respective open reading  
 608 frame (orf) were subcloned into pGEX-4T-1. Similarly, FHL1A cDNA was subcloned  
 609 into the pET47b (+) and expressed as a 6xHis fusion protein. The following  
 610 oligonucleotides were used to amplify nsP3 and nsP3ΔHVD cDNAs (sense: 5'-  
 611 cccggaattcATGgcaccgtcgtaccgggtaa-3'; antisense: 5'-  
 612 ccgctcgagTCAtaactcgtcgtccgtgtctg-3') and FHL1A (sense: 5'-  
 613 ccggaattccATGgcggagaagtttgactgcc-3'; antisense: 5'-  
 614 ccgctcgagTTAcagcttttggcacagtc-3'). E.Coli strain BL21 Star (Invitrogen) was  
 615 transformed with recombinant expression vectors encoding GST-nsP3, GST-  
 616 nsP3ΔHVD or 6xHis-FHL1A recombinant proteins. Transformed bacteria were

induced with isopropylthio- $\beta$ -Dgalactoside (IPTG) for 3 hours at 37°C. Cells were collected by centrifugation and the pellets were resuspended in lysis buffer containing lysozyme (1 mg/mL), incubated 30 min at 4°C followed by three subsequent freeze-thawed cycles and sonication. The bacterial lysates were centrifuged at 13,000 r.p.m for 20 min and the supernatants were incubated with glutathione-Sepharose beads for GST-nsP3 and GST-nsP3 $\Delta$ HVD, or Ni-NTA column (Qiagen) for 6xHis-FHL1A. Column washing and recombinant protein elution were performed according to the manufacturer's instructions. Five  $\mu$ L of eluted GST fusion proteins and 3  $\mu$ L of Ni-NTA eluted 6xHis-FHL1A were analyzed by SDS-PAGE and proteins were visualized by Coomassie staining. For pull-down assay, GST, GST-nsP3 or GST-nsP3 $\Delta$ HVD bound beads were incubated with 6xHis-FHL1A for 1 hour at 4°C in presence of 100  $\mu$ M ZnSO<sub>4</sub>. The resin was washed extensively with a buffer containing 500 mM KCL. The beads were then resuspended in Laemmli buffer, resolved on SDS-PAGE and the presence of 6xHis-FHL1A was assessed by western blot using anti-FHL1 antibody.

**Genetic analysis, fibroblasts and myoblasts from Emery-Dreifuss muscular dystrophy patients.** Dermal fibroblasts and myoblasts were taken from 4 patients carrying *FHL1* gene mutations. *FHL1* gene was analyzed as previously reported <sup>6</sup> as they had, among other symptoms, features reminiscent of Emery-Dreifuss muscular dystrophy. Patients P1, P2 and P3 were previously reported <sup>6</sup> with detailed clinical description (respectively as patient F321-3, F997-8 and F1328-4) while patient P4 was not yet published. Briefly, patient P4 had myopathy with joint contractures, hypertrophic cardiomyopathy, vocal cords palsy, short stature, alopecia, skin abnormalities and facial dysmorphism. In this patient, *FHL1* analysis revealed an insertion of a full-length LINE-1 retrotransposon sequence together with poly A tail of unknown length (i.e.,?

thereafter) after 27 bp of the start of exon 4 (c.183\_184ins [LINE1;?; 171\_183]) that results at mRNA level in altered splicing with retention of 108 bp of the inserted LINE sequence leading to predicted premature termination codon and shorter FHL1A (Extended Data Fig. 7b).

**Ethics statement.** All materials (skin and/or muscle biopsies) from patients and controls included in this study were taken with the informed consent of the donors and with approval of the local ethical boards. All the procedures were followed alongside the usual molecular diagnostic procedure during patient follow-up, and in accordance with the ethical standards of the responsible national committee on human experimentation.

**In vivo studies.** Animals were housed in the Institut Pasteur animal facilities accredited by the French Ministry of Agriculture for performing experiments on live rodents. Work on animals was performed in compliance with French and European regulations on care and protection of laboratory animals (EC Directive 2010/63, French Law 2013-118, February 6th, 2013). All experiments were approved by the Ethics Committee #89 (and registered under the reference APAFIS#6954-2016091410257906 v2). Male mice either deficient for FHL1 (FHL1-null) or not (WT littermates) were obtained by crossing heterozygous females for FHL1<sup>45</sup> with WT male Black Swiss mice. Nine day-old male littermates, both FHL1-null and WT mice, were injected with CHIKV21 (10<sup>5</sup> PFU/20µl) by intradermal route and viral load was determined in tissues by day 7 post infection. Virus titers in tissue samples were determined on Vero E6 cells by tissue cytopathic infectious dose 50 (TCID<sub>50</sub>/g). For histology experiments, muscles were snap frozen in isopentane cooled by liquid



nitrogen for cryo-sectioning then processed for histological staining (hematoxylin and eosin) or immunolabelling.

**Transmission electron microscopy.** Cells were scrapped and fixed for 24 h in 1% glutaraldehyde, 4% paraformaldehyde, (Sigma, St-Louis, MO) in 0.1 M phosphate buffer (pH 7.2). Samples were then washed in phosphate-buffered saline (PBS) and post-fixed for 1 h by incubation with 2% osmium tetroxide (Agar Scientific, Stansted, UK). Cells were then fully dehydrated in a graded series of ethanol solutions and propylene oxide. Impregnation step was performed with a mixture of (1:1) propylene oxide/Epon resin (Sigma) and then left overnight in pure resin. Samples were then embedded in Epon resin (Sigma), which was allowed to polymerize for 48 hours at 60°C. Ultra-thin sections (90 nm) of these blocks were obtained with a Leica EM UC7 ultramicrotome (Wetzlar, Germany). Sections were stained with 2% uranyl acetate (Agar Scientific), 5% lead citrate (Sigma) and observations were made with a transmission electron microscope (JEOL 1011, Tokyo, Japan).

**Cell viability assay.** Cell viability and proliferation were assessed using the CellTiter-Glo 2.0 Assay (Promega) according to the manufacturer's protocol. In brief, cells were plated in 48-well plates ( $3 \times 10^4$ ). At specific times, 100  $\mu$ l of CellTiter-Glo reagent were added to each well. After 10 min incubation, 200  $\mu$ l from each well were transferred to an opaque 96-well plate (Cellstar, Greiner bio-one) and luminescence was measured on a TriStar2 LB 942 (Berthold) with 0.1 second integration time.

**Statistical analysis.** Graphical representation and statistical analyses were performed using Prism7 software (GraphPad Software). Unless otherwise stated, results are

692 shown as means +/- standard deviation (SD) from at least 2 independent experiments  
693 in duplicates. Differences were tested for statistical significance using the unpaired  
694 two-tailed *t* test, One-way or Two-way Anova with multiple comparison post-test.

695

- 697 1. Burt, F. J. *et al.* Chikungunya virus: an update on the biology and pathogenesis of this  
698 emerging pathogen. *Lancet Infect. Dis.* **17**, e107–e117 (2017).
- 699 2. Silva, L. A. & Dermody, T. S. Chikungunya virus: epidemiology, replication, disease  
700 mechanisms, and prospective intervention strategies. *J. Clin. Invest.* **127**, 737–749 (2017).
- 701 3. Weaver, S. C., Charlier, C., Vasilakis, N. & Lecuit, M. Zika, Chikungunya, and Other  
702 Emerging Vector-Borne Viral Diseases. *Annu. Rev. Med.* **69**, 395–408 (2018).
- 703 4. Greene, W. K., Baker, E., Rabbitts, T. H. & Kees, U. R. Genomic structure, tissue  
704 expression and chromosomal location of the LIM-only gene, SLIM1. *Gene* **232**, 203–207  
705 (1999).
- 706 5. Schessl, J., Feldkirchner, S., Kubny, C. & Schoser, B. Reducing body myopathy and  
707 other FHL1-related muscular disorders. *Semin. Pediatr. Neurol.* **18**, 257–263 (2011).
- 708 6. Gueneau, L. *et al.* Mutations of the FHL1 gene cause Emery-Dreifuss muscular  
709 dystrophy. *Am. J. Hum. Genet.* **85**, 338–353 (2009).
- 710 7. Ooi, Y. S., Stiles, K. M., Liu, C. Y., Taylor, G. M. & Kielian, M. Genome-wide RNAi  
711 screen identifies novel host proteins required for alphavirus entry. *PLoS Pathog.* **9**, e1003835  
712 (2013).
- 713 8. Karlas, A. *et al.* A human genome-wide loss-of-function screen identifies effective  
714 chikungunya antiviral drugs. *Nat. Commun.* **7**, 11320 (2016).
- 715 9. Zhang, R. *et al.* Mxra8 is a receptor for multiple arthritogenic alphaviruses. *Nature*  
716 **557**, 570–574 (2018).
- 717 10. Tanaka, A. *et al.* Genome-Wide Screening Uncovers the Significance of N-Sulfation  
718 of Heparan Sulfate as a Host Cell Factor for Chikungunya Virus Infection. *J. Virol.* **91**, 1\_22  
719 (2017).
- 720 11. Shalem, O. *et al.* Genome-scale CRISPR-Cas9 knockout screening in human cells.  
721 *Science* **343**, 84–87 (2014).
- 722 12. Schuffenecker, I. *et al.* Genome microevolution of chikungunya viruses causing the  
723 Indian Ocean outbreak. *PLoS Med.* **3**, e263 (2006).
- 724 13. Li, W. *et al.* MAGeCK enables robust identification of essential genes from genome-  
725 scale CRISPR/Cas9 knockout screens. *Genome Biol.* **15**, 554 (2014).
- 726 14. Shathasivam, T., Kislinger, T. & Gramolini, A. O. Genes, proteins and complexes: the  
727 multifaceted nature of FHL family proteins in diverse tissues. *J. Cell. Mol. Med.* **14**, 2702–  
728 2720 (2010).
- 729 15. Brown, S. *et al.* Characterization of two isoforms of the skeletal muscle LIM protein  
730 1, SLIM1. Localization of SLIM1 at focal adhesions and the isoform slimmer in the nucleus  
731 of myoblasts and cytoplasm of myotubes suggests distinct roles in the cytoskeleton and in  
732 nuclear-cytoplasmic communication. *J. Biol. Chem.* **274**, 27083–27091 (1999).
- 733 16. Krempler, A., Kollers, S., Fries, R. & Brenig, B. Isolation and characterization of a  
734 new FHL1 variant (FHL1C) from porcine skeletal muscle. *Cytogenet. Cell Genet.* **90**, 106–  
735 114 (2000).
- 736 17. Pen, A. E. *et al.* A novel single nucleotide splice site mutation in FHL1 confirms an  
737 Emery-Dreifuss plus phenotype with pulmonary artery hypoplasia and facial dysmorphism.  
738 *Eur. J. Med. Genet.* **58**, 222–229 (2015).
- 739 18. Chan, K. K. *et al.* Molecular cloning and characterization of FHL2, a novel LIM  
740 domain protein preferentially expressed in human heart. *Gene* **210**, 345–350 (1998).
- 741 19. Rezza, G., Chen, R. & Weaver, S. C. O'nyong-nyong fever: a neglected mosquito-  
742 borne viral disease. *Pathog. Glob. Health* **111**, 271–275 (2017).
- 743 20. Couderc, T. *et al.* A mouse model for Chikungunya: young age and inefficient type-I  
744 interferon signaling are risk factors for severe disease. *PLoS Pathog.* **4**, e29 (2008).

21. Roberts, G. C. *et al.* Evaluation of a range of mammalian and mosquito cell lines for use in Chikungunya virus research. *Sci. Rep.* **7**, 14641 (2017).
22. Scholte, F. E. M. *et al.* Stress granule components G3BP1 and G3BP2 play a proviral role early in Chikungunya virus replication. *J. Virol.* **89**, 4457–4469 (2015).
23. Kim, D. Y. *et al.* New World and Old World Alphaviruses Have Evolved to Exploit Different Components of Stress Granules, FXR and G3BP Proteins, for Assembly of Viral Replication Complexes. *PLoS Pathog.* **12**, e1005810 (2016).
24. Jose, J., Taylor, A. B. & Kuhn, R. J. Spatial and Temporal Analysis of Alphavirus Replication and Assembly in Mammalian and Mosquito Cells. *mBio* **8**, 1–16 (2017).
25. Götte, B., Liu, L. & McInerney, G. M. The Enigmatic Alphavirus Non-Structural Protein 3 (nsP3) Revealing Its Secrets at Last. *Viruses* **10**, 1–26 (2018).
26. Meshram, C. D. *et al.* Multiple Host Factors Interact with Hypervariable Domain of Chikungunya Virus nsP3 and Determine Viral Replication in Cell-Specific Mode. *J. Virol.* (2018). doi:10.1128/JVI.00838-18
27. Mutso, M. *et al.* Mutation of CD2AP and SH3KBP1 Binding Motif in Alphavirus nsP3 Hypervariable Domain Results in Attenuated Virus. *Viruses* **10**, (2018).
28. Schessl, J. *et al.* Proteomic identification of FHL1 as the protein mutated in human reducing body myopathy. *J. Clin. Invest.* **118**, 904–912 (2008).
29. Bonne, G., Leturcq, F. & Ben Yaou, R. Emery-Dreifuss Muscular Dystrophy. in *GeneReviews®* (eds. Adam, M. P. *et al.*) (University of Washington, Seattle, 1993).
30. Frolov, I., Kim, D. Y., Akhrymuk, M., Mobley, J. A. & Frolova, E. I. Hypervariable Domain of Eastern Equine Encephalitis Virus nsP3 Redundantly Utilizes Multiple Cellular Proteins for Replication Complex Assembly. *J. Virol.* **91**, (2017).
31. Uversky, V. N. Intrinsically disordered proteins in overcrowded milieu: Membraneless organelles, phase separation, and intrinsic disorder. *Curr. Opin. Struct. Biol.* **44**, 18–30 (2017).
32. Nikolic, J. *et al.* Negri bodies are viral factories with properties of liquid organelles. *Nat. Commun.* **8**, 58 (2017).
33. Fros, J. J. *et al.* Chikungunya Virus nsP3 Blocks Stress Granule Assembly by Recruitment of G3BP into Cytoplasmic Foci. *J. Virol.* **86**, 10873–10879 (2012).
34. Remenyi, R. *et al.* Persistent Replication of a Chikungunya Virus Replicon in Human Cells Is Associated with Presence of Stable Cytoplasmic Granules Containing Nonstructural Protein 3. *J. Virol.* **92**, (2018).
35. Kadrmas, J. L. & Beckerle, M. C. The LIM domain: from the cytoskeleton to the nucleus. *Nat. Rev. Mol. Cell Biol.* **5**, 920–931 (2004).
36. Sheikh, F. *et al.* An FHL1-containing complex within the cardiomyocyte sarcomere mediates hypertrophic biomechanical stress responses in mice. *J. Clin. Invest.* **118**, 3870–3880 (2008).
37. Raskin, A. *et al.* A novel mechanism involving four-and-a-half LIM domain protein-1 and extracellular signal-regulated kinase-2 regulates titin phosphorylation and mechanics. *J. Biol. Chem.* **287**, 29273–29284 (2012).
38. Medina, F. *et al.* Dengue virus: isolation, propagation, quantification, and storage. *Curr. Protoc. Microbiol.* **Chapter 15**, Unit 15D.2. (2012).
39. Meertens, L. *et al.* The TIM and TAM families of phosphatidylserine receptors mediate dengue virus entry. *Cell Host Microbe* **12**, 544–557 (2012).
40. Joung, J. *et al.* Genome-scale CRISPR-Cas9 knockout and transcriptional activation screening. *Nat. Protoc.* **12**, 828–863 (2017).
41. Pellet, J. *et al.* ViralORFeome: an integrated database to generate a versatile collection of viral ORFs. *Nucleic Acids Res.* **38**, D371–378 (2010).
42. Gläsker, S. *et al.* Virus replicon particle based Chikungunya virus neutralization assay

795 using Gaussia luciferase as readout. *Viol. J.* **10**, 235 (2013).  
796 43. Kümmerer, B. M., Grywna, K., Gläsker, S., Wieseler, J. & Drosten, C. Construction of  
797 an infectious Chikungunya virus cDNA clone and stable insertion of mCherry reporter genes  
798 at two different sites. *J. Gen. Virol.* **93**, 1991–1995 (2012).  
799 44. Plaskon, N. E., Adelman, Z. N. & Myles, K. M. Accurate strand-specific  
800 quantification of viral RNA. *PloS One* **4**, e7468 (2009).  
801 45. Domenighetti, A. A. *et al.* Loss of FHL1 induces an age-dependent skeletal muscle  
802 myopathy associated with myofibrillar and intermyofibrillar disorganization in mice. *Hum.*  
803 *Mol. Genet.* **23**, 209–225 (2014).  
804  
805

## **ACKNOWLEDGMENTS**

This study has received funding from the French Government's Investissement d'Avenir program, Laboratoire d'Excellence "Integrative Biology of Emerging Infectious Diseases" (grant n°ANR-10-LABX-62-IBEID), the "Investissements d'Avenir" program ANR-10-IHUB-0002, the ANR-15-CE15-00029 ZIKAHOST, Institut Pasteur, Inserm and European Research Council. Viruses were graciously provided by the Europe and Virus Archive, which has received funding from the European Union's Horizon 2020 research and innovation program under grant agreement No 653316. The authors thank Félix Rey, Olivier Schwartz, Nicolas Manel, Yves Gaudin, Jan Hellert, Marie-Laure Chaix, Stéphane Marot, Sylvain Chawki, Antoine Canat, Alessia Zamborlini, and Hugues de Thé for critical readings of the manuscript and helpful discussions. The authors thank Pierre Thouvenot and David Hardy for technical assistance and Ju Chen and Julius Bogomolovas from UC San Diego (CA, USA) for providing FHL1 knockout mice. The authors are grateful to Mike Diamond and Julie Fox (Washington University School of Medicine, Saint Louis, MO, USA) and Frederic Tangy (Institut Pasteur, France) for providing us with the anti-CHIKV 265 mAb and the alphavirus nsP1-4 constructs, respectively.

## **AUTHORS' CONTRIBUTIONS**

L.M. and A.A. conceived the study. L.M, M.L.H, T.C, V.K, A.B, L.B.M, C.D., M.L and A.A designed the experiments. L.M. performed the CRISPR-Cas9 screening and infection studies with L.B.M. M.L.H characterized the FHL1 and nsP3 interactions and performed the immunoprecipitation and western blot studies with the help of V.K. A.L. validated the FHL1 gRNA and generated the FHL1 knockout cells described in this study. A.B. performed the immunofluorescence microscopy experiments and infection

studies. L.M. and E.S.L. analyzed the gRNA sequencing and identified the hits. J.B.G and P.R. performed the EM experiments. C.D. and M.B performed the GST-pull experiments. B.M.K generated the CHIKV molecular clones described in this study and P.O.V provided key CHIKV reagents. L.P and X.L. provided the alphavirus strains and performed infection studies. T.C. and M.L. performed in vivo studies and provided expertise in the design of CHIKV experiments. S.R. performed virus titration assays and mice genotyping. T.G. performed immunofluorescence experiments in mice tissues with T.C. A.T.B, R.B.Y., L.G., R.J.M. and G.B provided myoblasts and fibroblasts from EDMD patients and the description of a new *FHL1* mutation in EDMD disease. L.M and AA wrote the initial manuscript draft, and the other authors contributed to editing into its final form.

## FIGURE LEGENDS

### Figure 1. FHL1 is important for infection by CHIKV and ONNV

**a**, Results of the CHIKV screen analyzed by MAGeCK. Each circle represents individual gene. Y-axis represents the significance of sgRNA enrichment of genes in the selected population compared to the non-selected control population. X-axis represents a random distribution of the genes. **b**, E2 protein expression in control or  $\Delta$ FHL1 cells infected with the CHIKV 21 strain (MOI of 10). **c**,  $\Delta$ FHL1 HAP1 cells were trans-complemented with FHL1A, B or C isoforms, infected with CHIKV 21 strain (MOI of 10) and stained for E2 protein expression at 48hpi. Data shown in **b** and **c** are mean  $\pm$  SD (3 experiments, n=6; one-way ANOVA with Dunnett's multiple comparisons test). **d**,  $\Delta$ FHL1 and control cells were inoculated with CHIKV-Ross (MOI of 10), CHIKV-Brazza (MOI of 10), CHIKV-20235 (MOI of 10), CHIKV-M (M-899) (MOI of 10) or CHIKV-37997 (MOI of 10) and analyzed at 24 (293T) or 48hpi (HAP1) for E2 expression. Data shown are mean  $\pm$  SD (4 experiments, n=8 excepted for CHIKV-37997 n=4; one-way ANOVA with Tukey's multiple comparisons test). **e-g**,  $\Delta$ FHL1 and control HAP1 cells were inoculated with O'nyong-nyong virus (ONNV) (MOI of 2), Mayaro virus (MAYV) (MOI of 50), Eastern equine encephalitis virus (EEEV) (MOI of 2), Sindbis virus (SINV), Semliki Forest Virus (SFV), Ross River virus (RRV), Western equine encephalitis virus (WEEV), Venezuelan equine encephalitis virus (VEEV), Dengue virus (DENV) (MOI of 0.4) or ZIKA virus (ZIKV) (MOI of 50). **e**, Infection was quantified 48hpi by flow cytometry using the anti-E2 3E4 or 265 CHIKV mAb or the anti-EEEV mAb 1A4B6 (2 experiments, n=4). **f**, Virus growth was assessed at day 4 pi using real-time RT-PCR. Serial dilutions of infected supernatants titrated using the TCID50 method were used as quantification standards for RT-PCR. Accordingly, results were expressed for each virus as "molecular equivalents of TCID50". Data



shown are representative of two experiments. **g**, DENV or ZIKV infection were assessed by flow cytometry 48hpi using the anti-E protein 4G2 mAb. (3 experiments, n=6). **e-g** Data shown are mean +/- SD and significance was calculated using a one-way ANOVA statistical test with a Tukey's multiple comparisons test. **h**, BeWo and HepG2 cells were transduced with FHL1A or a control vector and challenged with CHIKV21 (MOI of 5) or CHIKV- M-899 (MOI of 2). Infection was quantified two days later by flow cytometry using the 3E4 mAb. Data shown are mean +/- SD (2 experiments, n=4 excepted for BeWo cells infected with CHIKV21, 3 experiments, n=6; one-way ANOVA with Tukey's multiple comparisons test). n.s non-significant; \*\*\* p< 0.0001.

**Figure 2. FHL1 interacts with CHIKV nsP3 and is required for CHIKV RNA replication**

**a**, Control and  $\Delta$ FHL1 HAP1 cells were inoculated with CHIKV 21 (MOI of 10). At the indicated time points, cells were treated with trypsin to remove cell surface bound virus and viral RNA was quantified by qRT-PCR. Data shown are mean +/- SD (3 experiments, n=9; two-tailed t-test). **b**, Control or  $\Delta$ FHL1 293T cells were transfected with *in vitro* transcribed CHIKV-M RNA expressing gaussia luciferase (Gluc) and Gluc activity was monitored at the indicated time points. RLU, relative light units. Data shown are mean +/- SEM (3 experiments, n=12; multiple t-tests). **c**, Control or  $\Delta$ FHL1 293T cells were transfected with a replication-deficient mutant CHIKV (CHIKV-GAA) RNA expressing renilla luciferase (RLuc) and luc activity was monitored at the indicated time points. Data shown are mean +/- SEM (3 experiments, n=12; multiple t-tests). **d**, Control or  $\Delta$ FHL1 293T cells were transfected with a replication-competent (CHIKV-GDD) or a replicon-deficient mutant CHIKV (CHIKV-GAA) capped RNA

893 expressing RLuc . The RLuc activity was monitored as described in c. Data shown are  
894 mean  $\pm$  SEM (3 experiments, n=12; 2-way ANOVA with Tukey's multiple comparison  
895 test). **e**, negative stranded viral RNA quantification by qRT-PCR from samples  
896 collected in (**a**). Data shown are mean  $\pm$  SD (2 experiments, n=8; one-way ANOVA  
897 with a Tukey's multiple comparisons test). Dashed line represents the experimental  
898 background threshold. **f**, Control and  $\Delta$ FHL1 293T cells were inoculated with CHIKV  
899 21 (MOI of 50). (left panel) Representative images of infected cells stained with anti-  
900 dsRNA mAb at 6hpi. (right panel) Number of foci per cell was quantified using the Icy  
901 software (2 experiments, n=42 cells in control and n=45 cells in  $\Delta$ FHL1 cells; two-tailed  
902 t-test). **g**, Transmission electron microscopy of control and  $\Delta$ FHL1 HAP1 cells  
903 challenged with CHIKV21 (MOI of 100) at 24h post-infection. Left panel shows CPV-II  
904 structures containing attached nucleocapsids at their cytoplasmic side (white arrows)  
905 as well as viral particles at the cell surface (thin black arrows). Middle panels show  
906 replication spherules (arrowheads) together with viral particles (thin black arrows) at  
907 the plasma membrane. PM= Plasma membrane. (Bars, 200nm). **h**, Co-  
908 immunoprecipitation of endogenous FHL1 and CHIKV nsP3 from cell lysates of 293T  
909 cells infected with a CHIKV nsP3-mCherry reporter virus at MOI 5 or 50. **i**, *In vitro* co-  
910 immunoprecipitation analyzing the direct interaction between CHIKV-nsP3 and FHL1A  
911 through the HVD domain. GST-precipitation of GST-nsP3 or GST-nsP3 $\Delta$ HVD and  
912 immunoblot analysis of 6xHis-FHL1A. **j**, 293 T were co-transfected with plasmids  
913 encoding FHL1A-HA and FLAG-tagged CHIKV nsP3 WT or CHIKV nsP3  $\Delta$ HVD or  
914 CHIKV lacking the amino acid region 423-454 ( $\Delta$ R4). Cellular lysates were subject to  
915 immunoprecipitation with anti-FLAG beads followed by immunoblot analysis with anti-  
916 FLAG or anti-HA mAb. **k**, (left panel) Schematic representation of FHL1A protein in  
917 fusion with the nsP3 interacting region (FHL1A-R4) or a similar randomized sequence

(FHL1A-R4\*). (Right panel) Immunoassay of the interaction between CHIKV nsP3 and FHL1A fusion proteins in 293T cells co-transfected with FLAG-tagged CHIKV nsP3 and either a HA-tagged FHL1A, FHL1A-R4 or FHL1A-R4\* constructs. Cellular lysates were subject to immunoprecipitation with anti-FLAG followed by immunoblot analysis with anti-FLAG and anti-HA Ab. **I**,  $\Delta$ FHL1 293T cells were transfected with an empty vector or plasmids encoding FHL1A, FHL1A-R4 or FHL1A-R4\*. Cells were incubated with CHIKV21 (MOI of 5) and infection was quantified 24hpi by flow cytometry. Data shown are mean  $\pm$  SD (2 experiments, n=4; one-way ANOVA with Dunnett's multiple comparison test). \*\*  $P < 0.01$  \*\*\*\*  $P < 0.0001$ ; ns not significant.

**Figure 3. Primary myoblasts and fibroblasts from FHL1 deficient patients are resistant to CHIKV infection.**

**a**, FHL1 expression in primary myoblasts and fibroblasts from healthy donors or Emery-Dreifuss muscular dystrophy (EDMD) patients. CM: control myoblasts, PM: patient myoblasts; CF: control fibroblast, PF: patient fibroblasts. **b**, Cells from controls or EDMD patients were inoculated with CHIKV expressing nsP3-mCherry. At 48-hpi, cells were fixed and images were taken on fluorescence microscope. Images are representative of three experiments. **c**, E2 protein expression in primary cells from healthy controls or EDMD patients infected with CHIKV21 (MOI of 2). Data shown are mean  $\pm$  SD (2 experiments, n=4 for myoblast; 4 experiments, n=8 for fibroblast; one-way ANOVA with Tukey's multiple comparisons test). **d**, Quantification of viral particles released in supernatant of infected cells collected at 24, 48- and 72-hpi. FIU, flow cytometry infectious units. Data shown are mean  $\pm$  SEM (2 experiments, n=4 for myoblast; 3 experiments, n=6 for fibroblast; multiple t-test). **e**, Primary fibroblasts from a control (CF1) or two FHL1 null patients (PF2, PF4) were inoculated with CHIKV-

Ross, CHIKV-Brazza, CHIKV-H20235 strains or MAYV (MOI of 2) and analyzed for E2 expression. Data shown are mean  $\pm$  SD (3 experiments n=6, one-way ANOVA with Dunnett's multiple comparisons test). **f-g** Fibroblasts from control (CF1) or FHL1 null patients (PF2, PF4) were transduced with a lentiviral vector encoding FHL1A or a control vector and then challenged with CHIKV21 (MOI of 2). **f**, Infection was quantified as described in c. Data shown are mean  $\pm$  SD (2 experiments, n=4, one-way ANOVA with Tukey's multiple comparisons test). **g**, Supernatants were collected from infected cells at indicated time point and viral titers were measured on VeroE6 cells. Data shown are mean  $\pm$  SEM (2 experiments, n=4; two-way ANOVA with Dunnett's multiple comparisons test). \*P<0.05; \*\*P<0.01; \*\*\*\* P< 0.0001; ns not significant.

**Figure 4. FHL1 is a factor of susceptibility to CHIKV infection in mice.**

**a**, Viral titers in tissues of nine-day-old mice. WT littermates (n=5) and FHL1-null mice (n=7) were inoculated with  $10^5$  PFU of CHIKV via the ID route and sacrificed by 7 days post infection. The amount of infectious virus in tissues was quantified by TCID<sub>50</sub>. The broken line indicates the detection threshold. **b**, Hematoxylin and eosin staining of transversal section of skeletal muscle in CHIKV-infected mice. **c**, Immunostaining of nuclei, FHL1, vimentin and CHIKV antigens on skeletal muscle of CHIKV-infected mice. \*\* P<0.01; ns not significant.

## Extended Data Figures

### Extended Data Fig. 1. CRISPR-Cas9 genetic screen identified essential host factors of CHIKV infection

**a**, Schematic of CRISPR-Cas9 genome-wide screen in HAP1 haploid cells. **b**, Ranked list of the top 30 genes identified using MAGeCKs algorithm and their corresponding rank in RIGER analysis. **c**, Venn diagram comparing the top 200 hits from our screen and previous CRISPR and haploid screens for CHIKV host factors.

### Extended Data Fig. 2. Validation of FHL1 gene edition by CRISPR-Cas9

Schematic of the genomic organization of FHL1 (**a**), alternative splicing of the isoforms FHL1A, FHL1B and FHL1C (**b**) and their corresponding proteins (**c**). Initiation and stop codon are indicated in red and relative positions of the sequence targeted by the sgRNA are indicated in blue. **d**, Sanger sequencing of FHL1 in control and  $\Delta$ FHL1 HAP1 cells. **e**, Genomic DNA was used for PCR amplification using primers flanking the sequence targeted by FHL1 sgRNA2. The absence of an amplification product of 3.9 kb (black arrow) in HAP1 clone suggests that a large indel is responsible for the absence of FHL1 expression. Asterisk: unspecific PCR products. **f**, Immunoblot of FHL1 in control and  $\Delta$ FHL1 cells. One representative of three experiments is shown. **g**, Control and  $\Delta$ FHL1 cells were plated and viability was assessed over a 72 hours period using the CellTiter-Glo assay. Data shown are mean  $\pm$  SEM (2 experiments, n=8; two-way ANOVA with Dunnett's multiple comparisons test). \*P<0.05; ns not significant.

**Extended Data Fig. 3. FHL1 is an essential host factor for CHIKV and ONNV infection**

**a**, Immunofluorescence images of control and  $\Delta$ FHL1 HAP1 cells inoculated with CHIKV21 (MOI of 10), fixed 48 hpi and stained for E2 expression. **b**, Immunofluorescence images of control and  $\Delta$ FHL1 HAP1 cells inoculated with CHIKV expressing nsP3-mCherry (MOI of 10) and fixed 48 hpi. **a**, **b**, Images were taken on fluorescence microscope and are representative of three experiments. **c**, Control and  $\Delta$ FHL1 HAP1 cells were inoculated with increasing MOI of CHIKV21, and infection was quantified 48hpi by flow cytometry using the anti-E2 3E4 mAb. Data shown are mean  $\pm$  SD (3 experiments, n=6; two-way ANOVA with Tukey's multiple comparison test). **d**, Multi-step growth curves with CHIKV 21 strain in control or  $\Delta$ FHL1 cells. Data shown are mean  $\pm$  SEM (2 experiments, n=4; multiple t-tests). **e**, Control and  $\Delta$ FHL1 HAP1 cells were inoculated with increasing MOI of ONNV or MAYV, and Infection was quantified 48hpi by flow cytometry using anti-E2 3E4 and 265 mAbs. Data shown are mean  $\pm$  SEM (2 experiments, n=4; two-way ANOVA with Tukey's multiple comparisons test). **f**, Control and  $\Delta$ FHL1 HAP1 cells were inoculated with increasing MOI of DENV or ZIKV, and infection was quantified 48hpi by flow cytometry using the anti-E 4G2 mAb. Data shown are mean  $\pm$  SEM (3 experiments, n=6; two-way ANOVA with Tukey's multiple comparisons test). \* P< 0.05; \*\*\*\* P< 0.0001; ns not significant.

**Extended Data Fig. 4. FHL1A and FHL2 ectopic expression in  $\Delta$ FHL1 cells restores CHIKV infection**

**a**, Immunoblot of ectopic FHL1 expression in HAP1 cells stably transduced with an empty vector or FHL1A, FHL1B or FHL1C isoform. **b**, Quantification in the supernatant

of infected HAP1 cells of viral particles released by measuring viral titer on Vero E6 cells. Data shown are representative of 3 experiments, mean +/- SEM. **c**, ΔFHL1 293T cells transfected with an empty vector or HA-tagged plasmids encoding FHL1A and FHL2 were subjected to infection with increasing MOI of CHIKV21. Infection was quantified 24hpi by flow cytometry. Data shown are mean +/- SD (3 experiments, n=6; two-way ANOVA with Dunnett 's multiple comparison test) \*\*P<0.01; \*\*\*\* P< 0.0001; ns not significant.

**Extended Data Fig. 5. FHL1A overexpression in BeWo and HepG2 cells enhances CHIKV infection**

**a**, Expression of endogenous FHL1 in HAP1, 293T, BeWo and HepG2. **b**, Immunoblot of ectopic FHL1 expression in Bewo and HepG2 cells stably transduced with an empty vector or HA-tagged FHL1A. **c** and **d**, Bewo cells stably transduced with an empty vector or HA-tagged FHL1A were inoculated with increasing MOI of CHIKV21. **c**, Infection was quantified 48hpi by flow cytometry using the anti-E2 3E4 mAb. Data shown are mean +/- SEM (3 experiments, n=6; Two-way ANOVA with Tukey's multiple comparisons test). **d**, Quantification in the supernatants of infected cells of viral particles released by measuring viral titer on Vero E6 cells. Data shown are mean +/- SD (2 experiments, n=4; two-tailed t-test). **e**, HepG2 cells stably transduced with an empty vector or FHL1A were inoculated with increasing MOI of CHIKV-M-Gluc. Infection was quantified 48hpi as indicated in c. Data shown are mean +/- SEM (2 experiments, n=4; Two-way ANOVA with Tukey's multiple comparisons test). \*\* P<0.001; \*\*\*\* P< 0.0001; ns not significant.

**Extended Data Fig. 6. CHIKV nsP3 directly interacts with FHL1A and FHL2**

1038 **a**, Control or  $\Delta$ FHL1 HAP1 cells were transfected with CHIKV-M-Gluc capped genomic  
1039 RNA expressing Gaussia luciferase (Gluc). Gluc activity was monitored at indicated  
1040 time point. RLU, relative light units. Data shown are mean +/- SEM (3 experiments,  
1041 n=12; multiple t-tests). **b**, Confocal microscopy of the colocalization of CHIKV nsP3  
1042 with FHL1 protein in fibroblasts inoculated with CHIKV-nsP3-mCherry (MOI of 2), fixed  
1043 48 hpi and stained with anti-FHL1. Images are representative of three experiments. **c**,  
1044 Immunoassay of the interaction between CHIKV nsP3 and FHL1 isoforms in 293T cells  
1045 transfected with FLAG-tagged CHIKV nsP3 and either an empty vector or plasmids  
1046 encoding the three HA-tagged FHL1 isoforms. Cellular lysates were subject to  
1047 immunoprecipitation with anti-FLAG followed by immunoblot analysis with anti-FLAG  
1048 and anti-HA. **d**, Immunoassay of the interaction between CHIKV nsP3 and FHL2 in  
1049 293T cells transfected with FLAG-tagged CHIKV nsP3 and either an empty vector or  
1050 plasmids encoding HA-tagged FHL1 and FHL2. Cellular lysates were subject to  
1051 immunoprecipitation with anti-FLAG followed by immunoblot analysis with anti-FLAG  
1052 and anti-HA. **e**, Endogenous FHL1, G3BP1 or G3BP2 immunoprecipitation from  
1053 control and  $\Delta$ FHL1 293T cells transfected with plasmids encoding FLAG-tagged  
1054 CHIKV, Sindbis (SINV) or Semliki forest virus (SFV) nsP3. Cellular lysates were  
1055 subject to immunoprecipitation with anti-FLAG followed by immunoblot analysis with  
1056 anti-FLAG, anti-FHL1, anti-G3BP1 and anti-G3BP2. **f**, Endogenous FHL1  
1057 immunoprecipitation from 293T cells transfected with plasmids encoding FLAG-tagged  
1058 full length CHIKV nsP3, CHIKV nsP3 carrying the SINV HVD (CHIKV/HVD-SIV) or  
1059 Sindbis nsP3 carrying CHIKV HVD (SINV/HVD-CHIKV). Cellular lysates were  
1060 subjected to immunoprecipitation with anti-FLAG followed by immunoblot analysis with  
1061 anti-FLAG and anti-FHL1. **g**, Purified GST-tagged nsP3 constructs and HA-tagged



1062 FHL1A detected by coomassie blue staining. **c-i**, One experiment representative of  
1063 three is shown. \*P<0.05; \*\*P<0.01; \*\*\*\* P< 0.0001; ns not significant.

1064

1065 **Extended Data Fig. 7. Mapping the FHL1–nsP3 interaction**

1066 **a**, The sequence alignment of nsP3 protein HVD domains of representative members  
1067 of New and Old World alphaviruses. Sequence alignment was performed with Clustall  
1068 Omega and edited with Jalview. R1, R2 and R3 sequences of high homology between  
1069 CHIKV strains and ONNV are defined by colored lines. CHIKV06-21 (GenBank  
1070 accession number AM258992.1); CHIKV Ross (GenBank accession number  
1071 MG280943.1); CHIKV H20235 (GenBank accession number MG208125.1); CHIKV  
1072 37997 (GenBank accession number AY726732.1); ONNV (GenBank accession  
1073 number MF409176.1); SFV (GenBank accession number HQ848388.1); MAYV  
1074 (GenBank accession number KY618137.1); SINV (GenBank accession number  
1075 MF409178.1); EEEV (GenBank accession number Q4QXJ8.2); VEEV (GenBank  
1076 accession number P27282.2). **b**, (top panel) Schematic representation of CHIKV nsP3  
1077 constructs deleted for the R1, R2, R3 or R4 sequences. (bottom panel) 293T cells were  
1078 transfected with FHL1A-HA and either an empty vector or plasmids encoding FLAG-  
1079 tagged nsP3 constructs. Cell lysates were immunoprecipitated with anti-FLAG  
1080 followed by immunoblot analysis with anti-HA or anti-FLAG Ab. One experiment  
1081 representative of three is shown. **c**, Alignment of nsP3 regions containing the WT R4  
1082 sequence or the corresponding randomized sequence. Dashes represents identical  
1083 aa. **d**, Control 293T cells were transfected with the indicated CHIKV capped in vitro  
1084 transcribed RNA expressing renilla luciferase (Rluc). Rluc activity was monitored at  
1085 indicated time points. RLU, relative light units. Data shown are mean +/- SEM (2

experiments, n=8; Two-way ANOVA with Tukey's multiple comparisons test). \*\*\*\* P< 0.0001; ns not significant.

#### **Extended Data Fig. 8. CHIKV Infection of myoblasts and fibroblasts derived from EDMD patients**

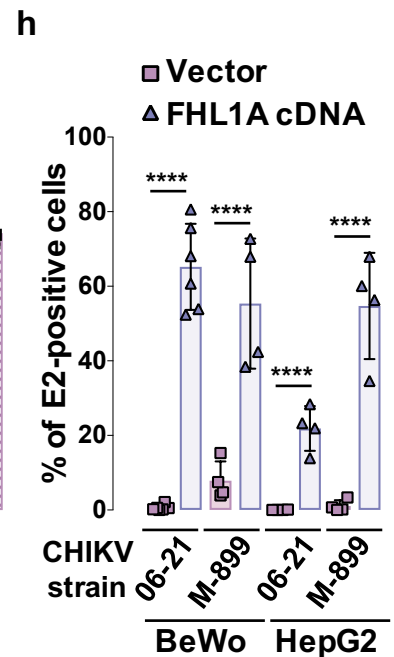
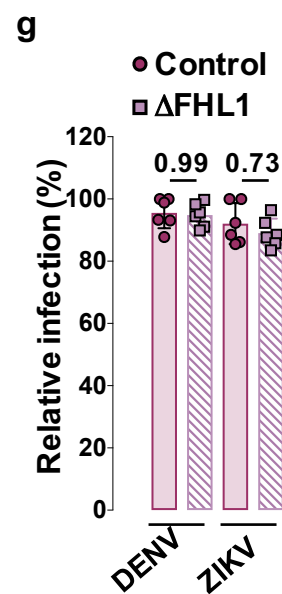
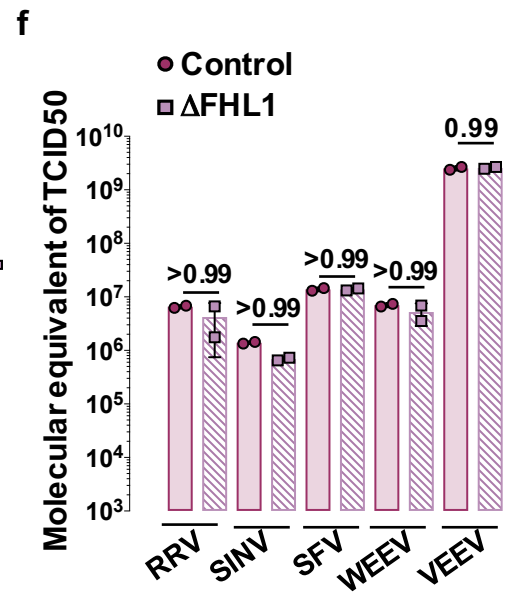
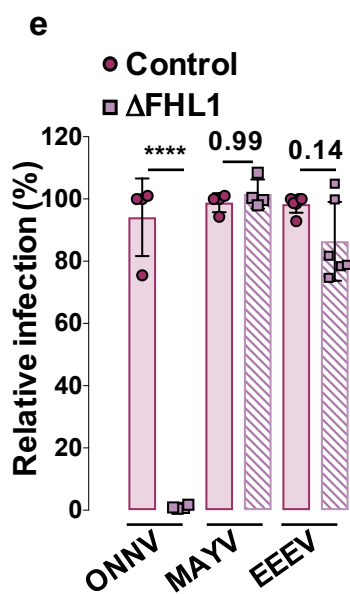
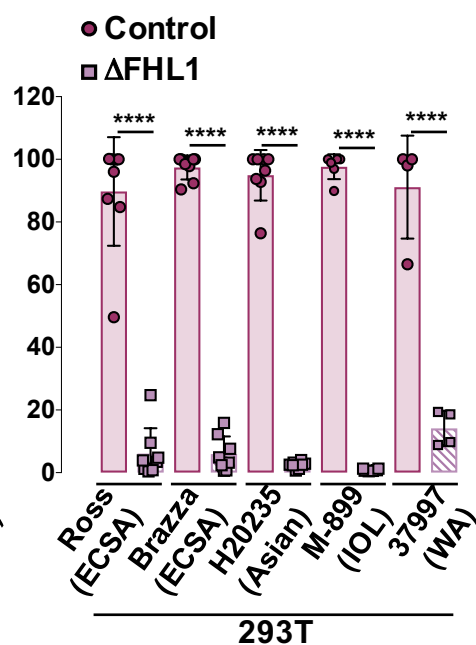
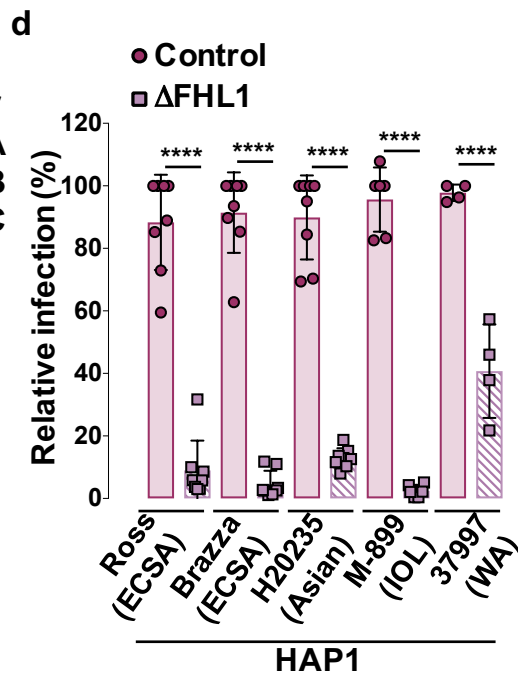
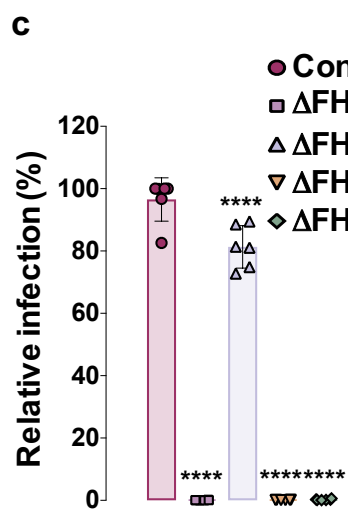
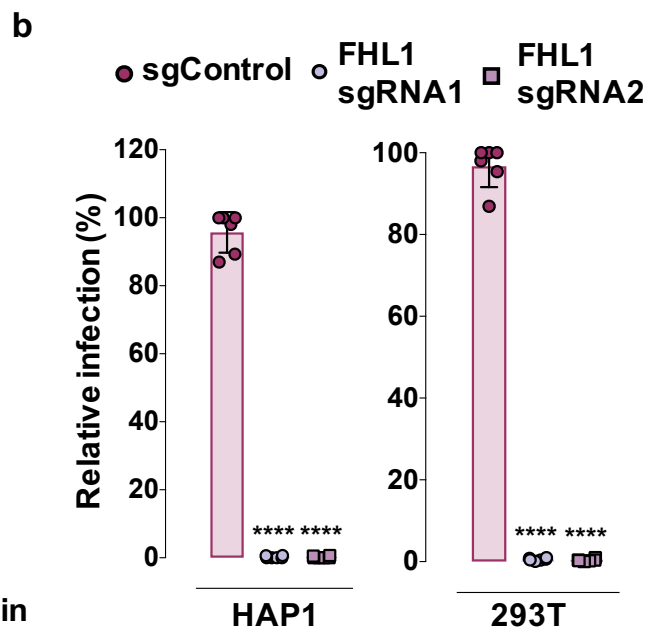
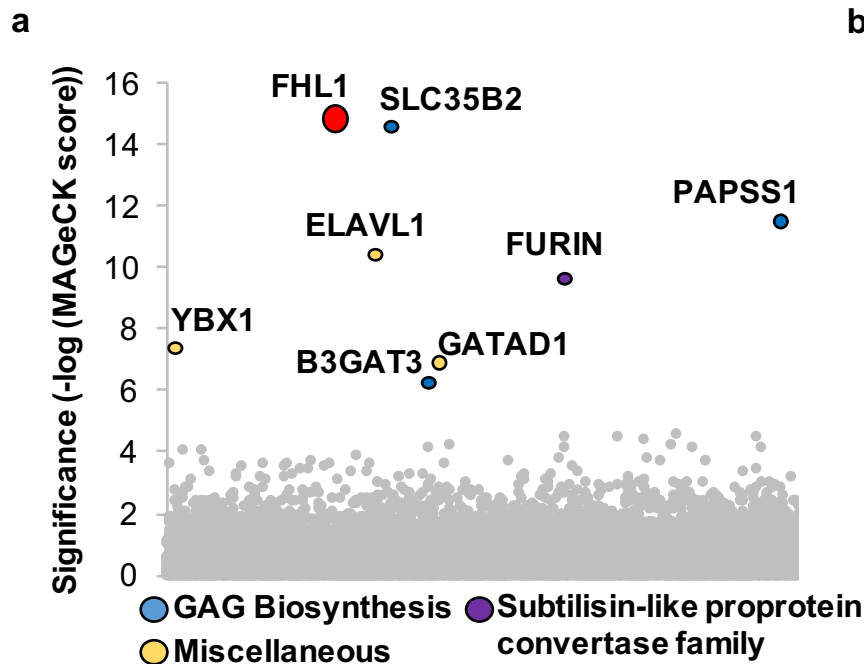
**a**, Schematic of FHL1A protein in three EDMD patient (P1, P2 and P3). **b**, Schematic of FHL1 genomic organization in newly described patient with a LINE1 insertion within exon 4 (P4). **c**, Myoblasts and fibroblasts from EDMD patients or healthy donors were infected with increasing MOI of CHIKV21, and infection was quantified 24hpi by flow cytometry using the anti-E2 3E4 mAb. Data shown are mean +/- SEM (2 experiments, n=4 for myoblast; 3 experiments, n=6 for fibroblast; Two-way ANOVA with Dunnett's multiple comparisons test). **d**, Fibroblasts from EDMD patients or healthy donors were inoculated with increasing MOI of CHIKV-Ross, CHIKV-Brazza, CHIKV-H20235, and infection was quantified 24hpi by flow cytometry using the anti-E2 3E4 mAb. Data shown are mean +/- SEM (3 experiments, n=6; two-way ANOVA with Dunnett's multiple comparisons test). **e**, Immunoblot of ectopic FHL1 expression in patient primary fibroblast (PF2 and PF4) cells stably transduced with an empty vector or a plasmid encoding HA-FHL1A. One representative of two experiments is shown. \*\*\*\* P< 0.0001; ns not significant.

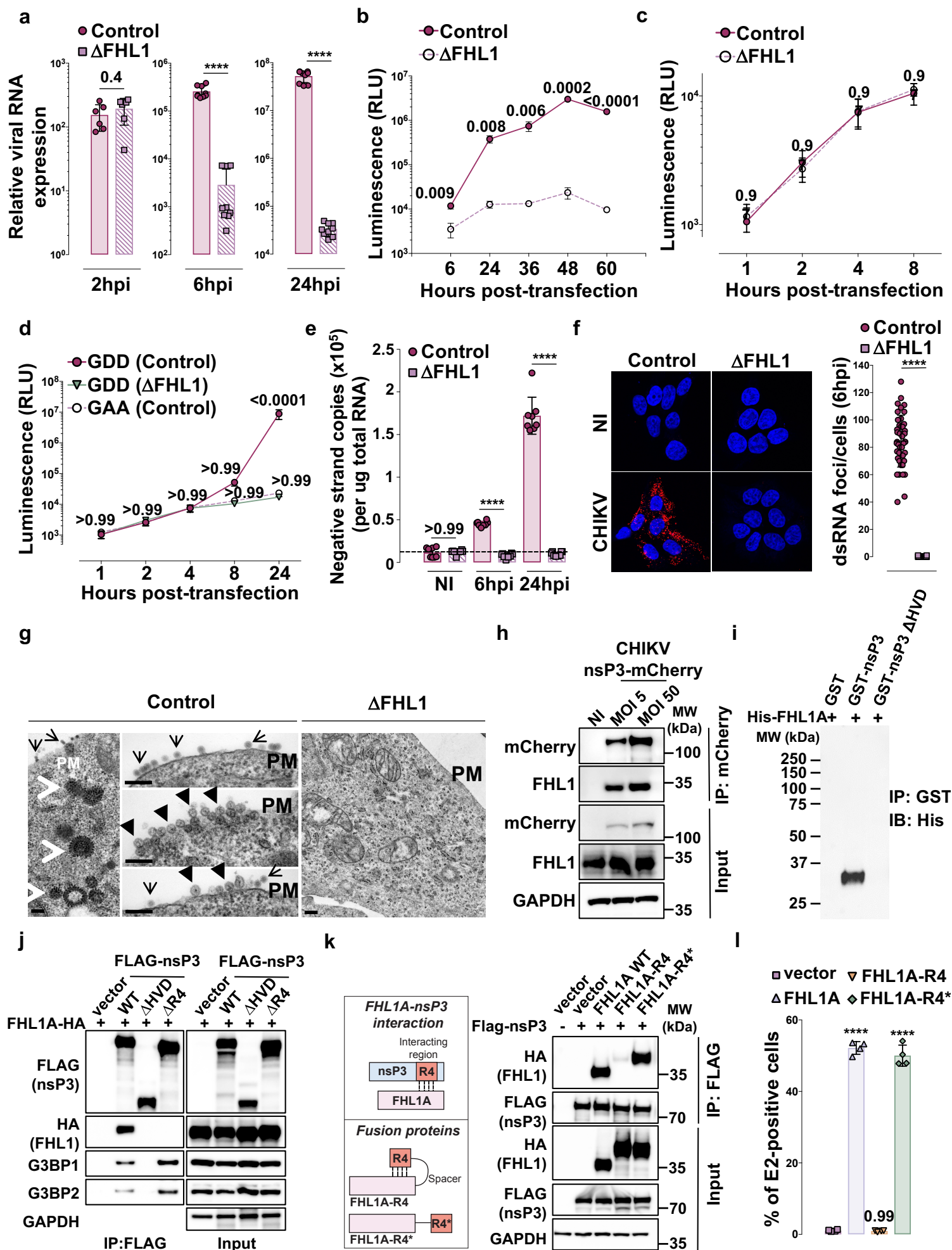
#### **Extended Data Fig.9. Mouse FHL1 interacts with CHIKV nsP3 and restores infection in $\Delta$ FHL1 cells**

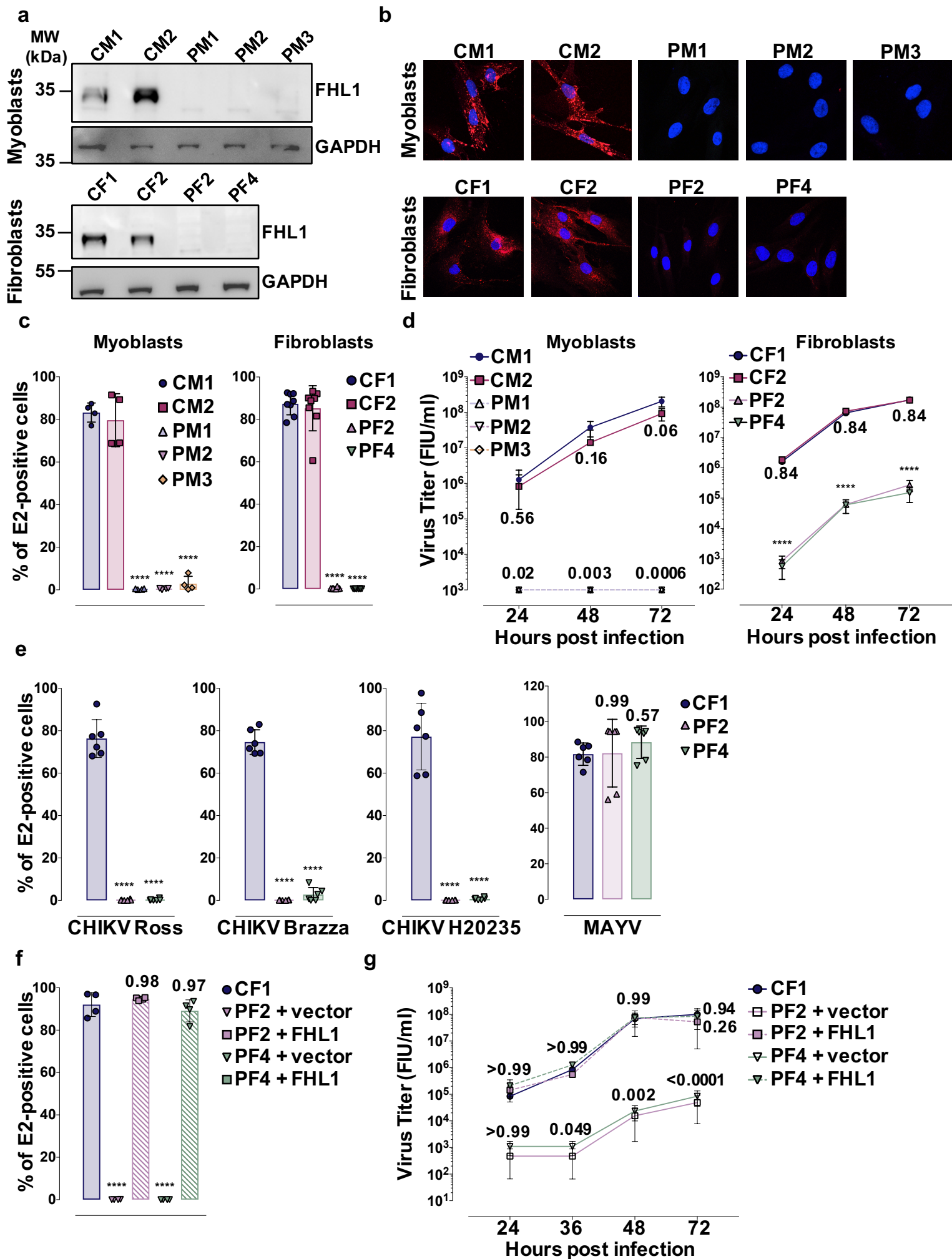
**a**, Sequence alignment of murine and human FHL1A proteins. **b**, 293T cells were co-transfected with FLAG-tagged CHIKV nsP3 and plasmids encoding HA-tagged mFHL1 or hFHL1A. Cellular lysates were subject to immunoprecipitation with anti-HA followed

1111 by immunoblot analysis with anti-FLAG (nsP3) and anti-HA (FHL1). **c**, Immunoblot of  
1112 FHL1 ectopic expression in  $\Delta$ FHL1 293T stably transduced with plasmid encoding  
1113 murine FHL1 (mFHL1) or human FHL1A (hFHL1A). **d**, Cells showed in **c** were  
1114 inoculated with increasing MOI of CHIKV21. Infection was quantified by flow cytometry  
1115 at 24 hpi using anti-E2 3E4 mAb. Data shown are mean  $\pm$ SD (3 experiments, n=6;  
1116 two-way ANOVA with Dunnett's multiple comparisons test). **e**, (left panel) Immunoblot  
1117 of endogenous FHL1 in control and  $\Delta$ FHL1 C2C12 murine cells. (right panel) Control  
1118 and  $\Delta$ FHL1 cells were inoculated with CHIKV21 or MAYV (MOI of 2) and infection was  
1119 quantified at 24hpi by flow cytometry using anti-E2 3E4 or anti-E2 265 mAb. One  
1120 representative of three experiments is shown. \*\*\*P<0.001; \*\*\*\*P<0.0001; ns not  
1121 significant.

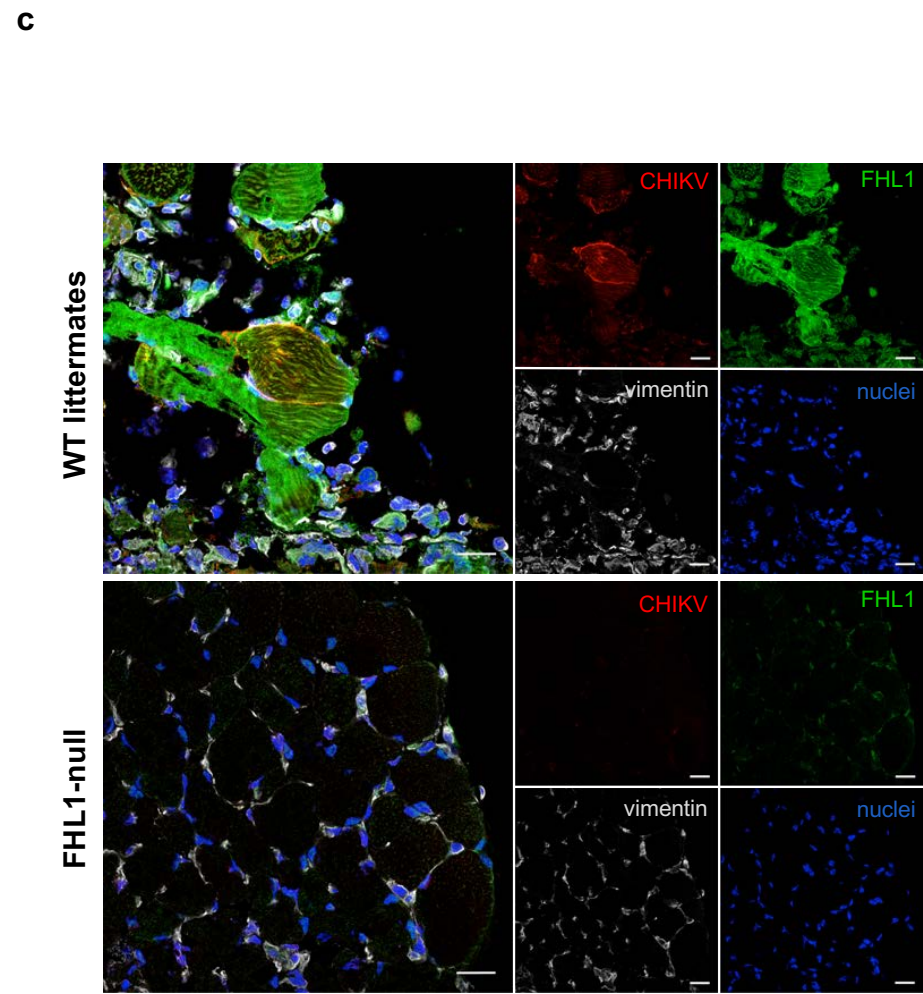
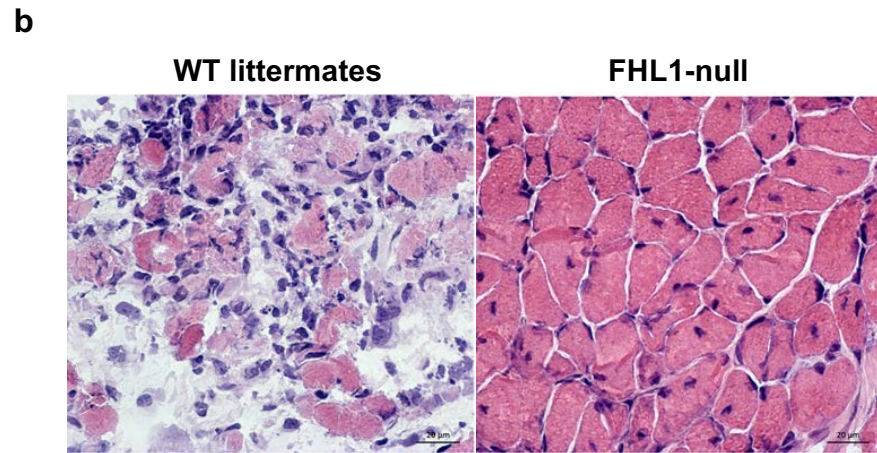
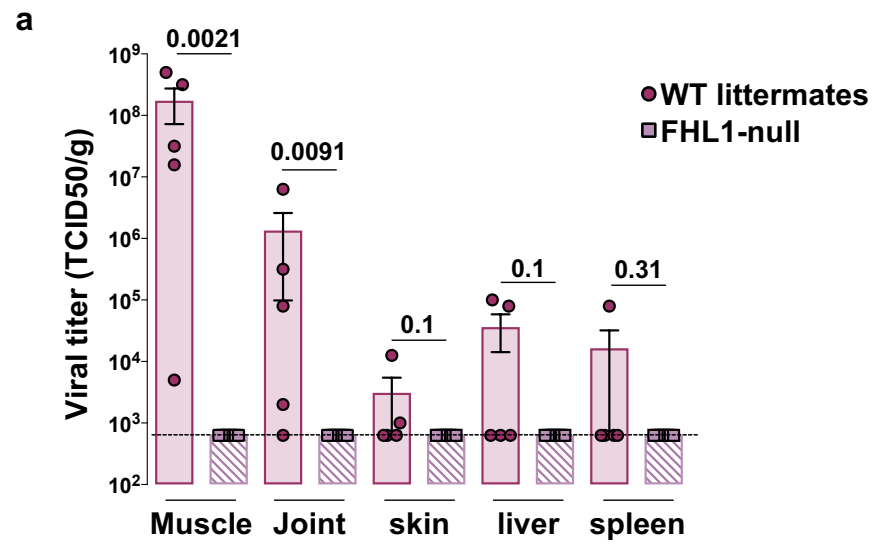
1122





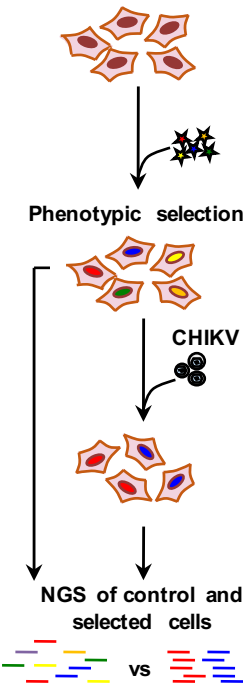






a

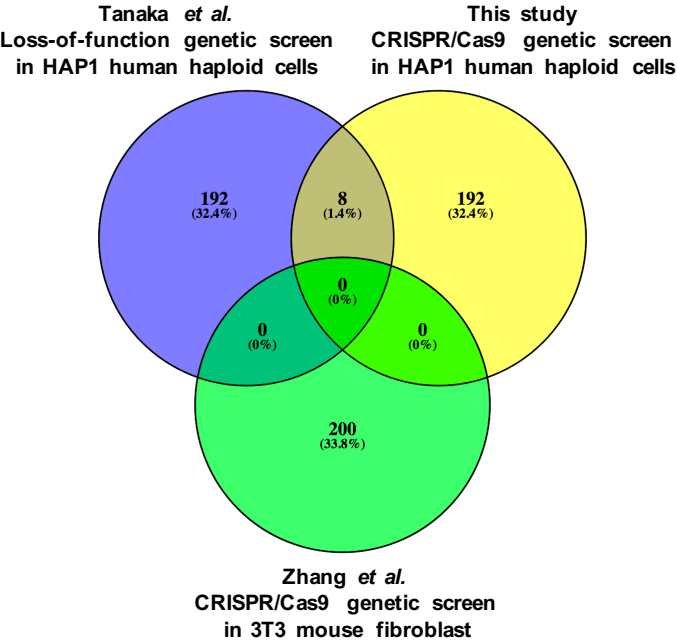
Transduction of HAP1 haploid cells  
with pooled lentiviral sgRNA  
library A or B



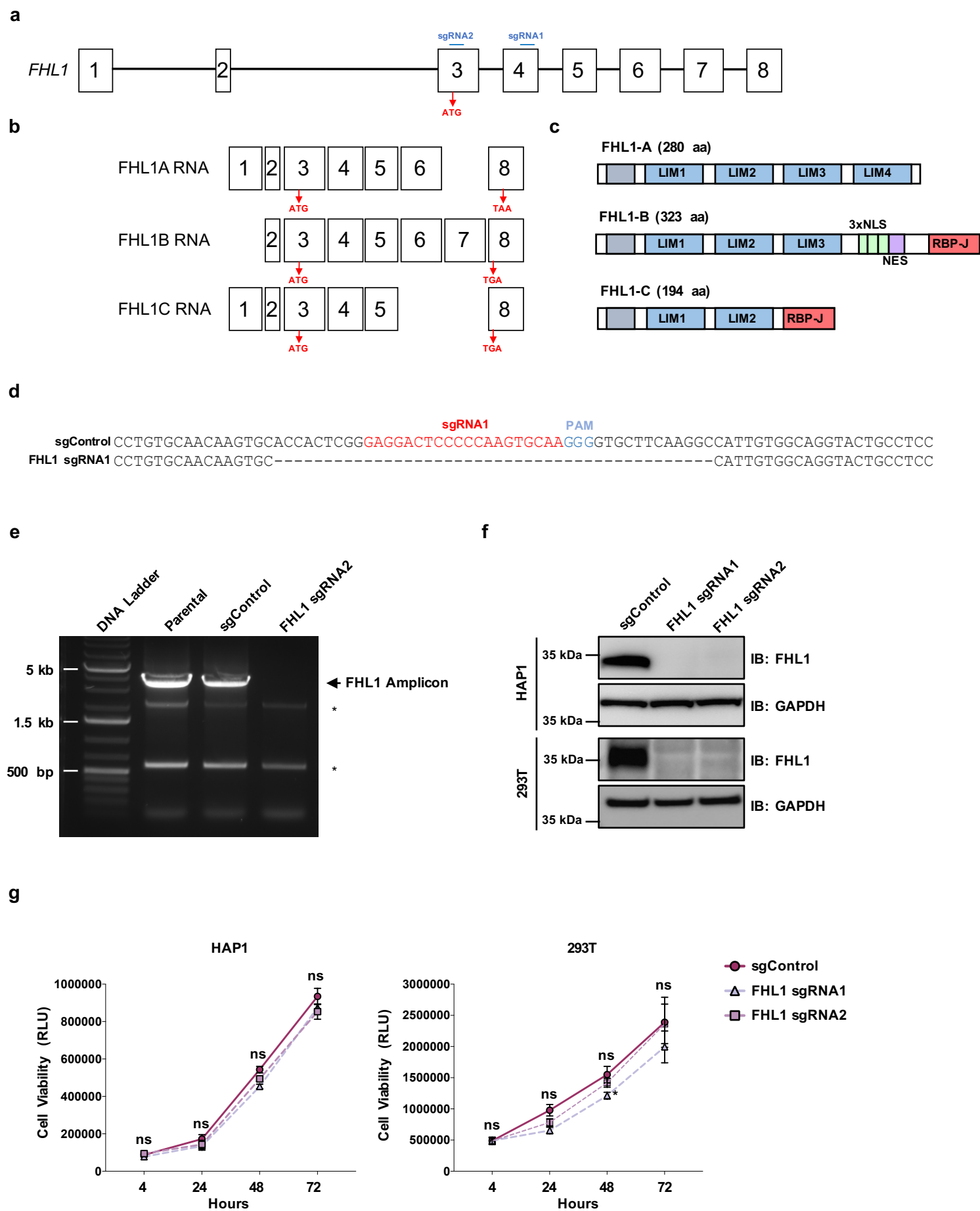
b

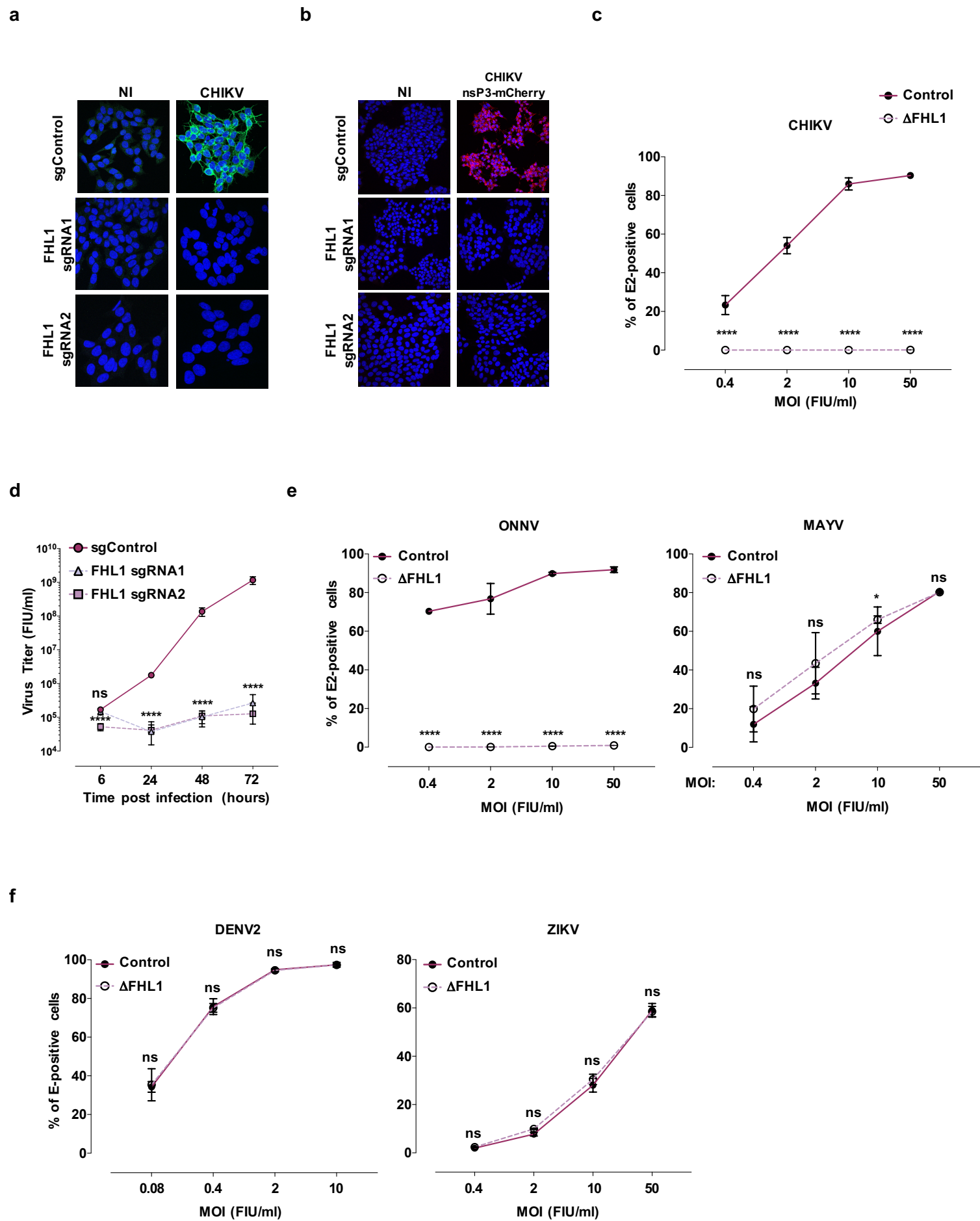
Ranked Genes	MAGeCK rank	RIGER Rank
FHL1	1	1
SLC35B2	2	2
PAPSS1	3	3
ELAVL1	4	4
FURIN	5	7
YBX1	6	6
GATAD1	7	5
B3GAT3	8	9
OR10W1	9	217
MTRNR2L5	11	18
COA5	12	436
POMT2	13	641
ELP5	14	47
PRIM2	16	337
NRCAM	17	238
PDE8B	18	78
EXT1	19	26
ELF2	20	10
MYT1L	21	381
CUL5	22	956
MAP4K3	23	37
ALDH18A1	24	107
ACTR10	25	13544
SLC7A6OS	26	2704
C11orf30	27	11
BID	28	8
SMOC1	30	507
SCGB1D1	32	84
RPE65	33	75
FAM124B	34	459

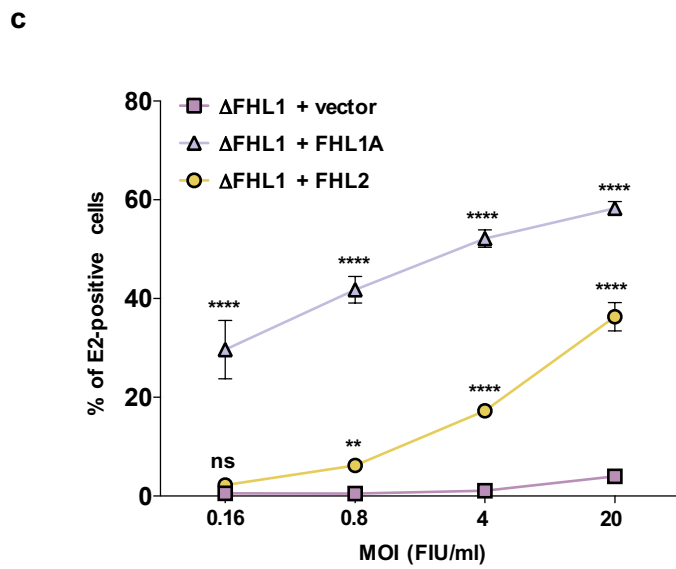
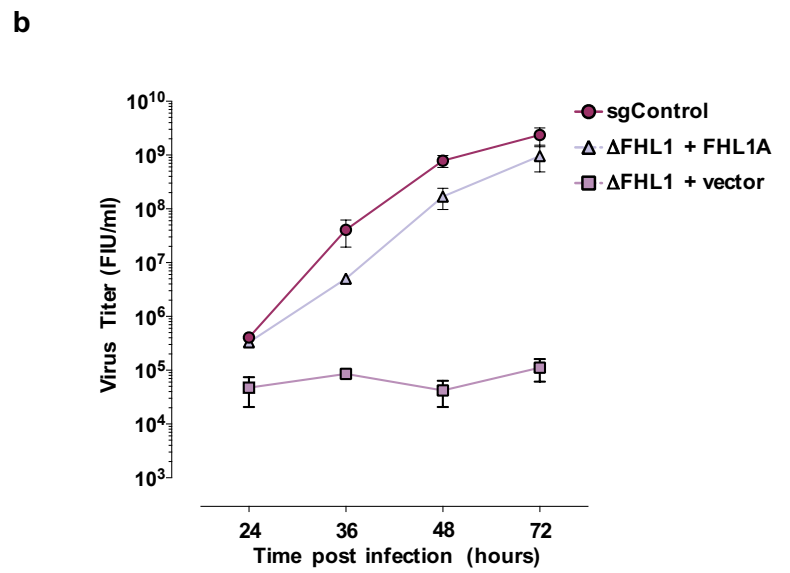
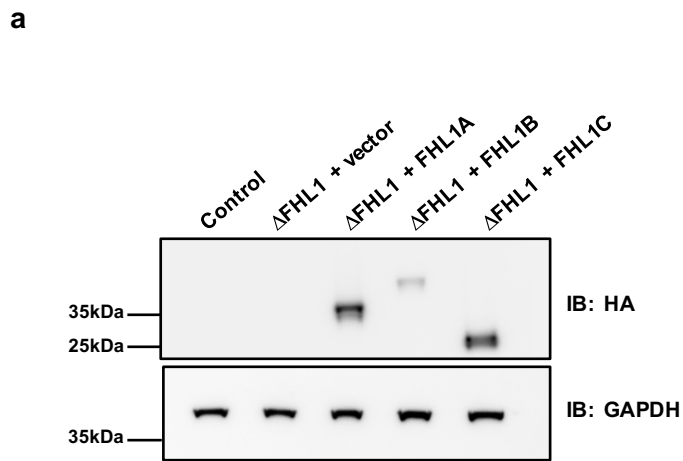
c

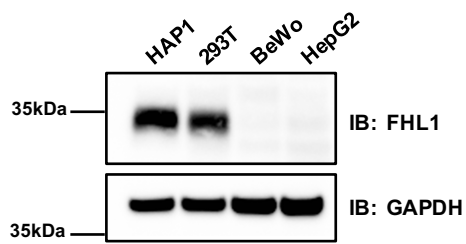
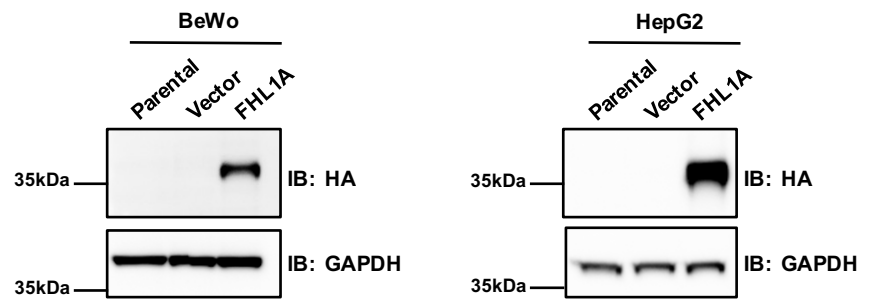
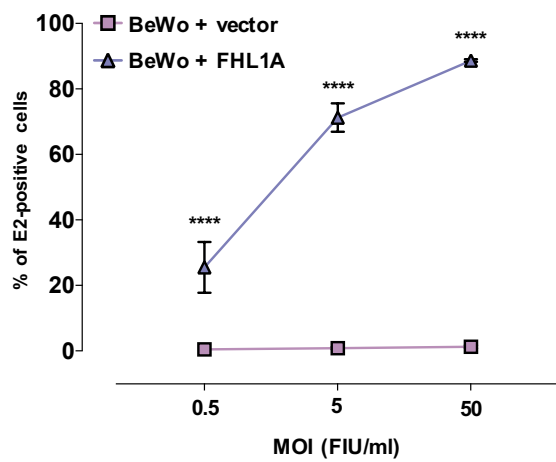
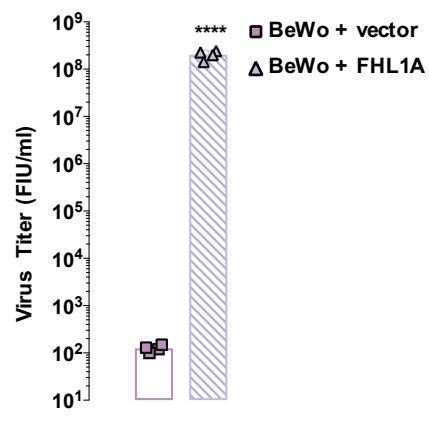
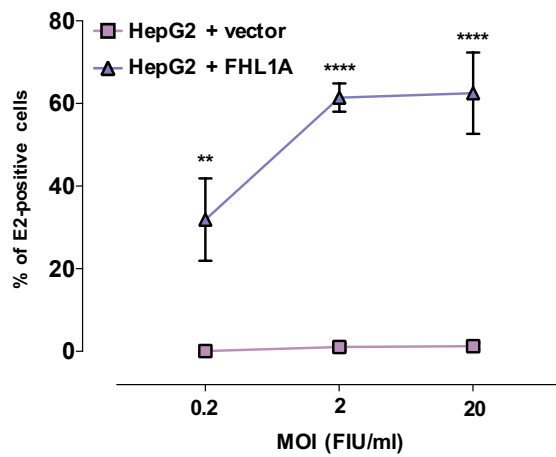


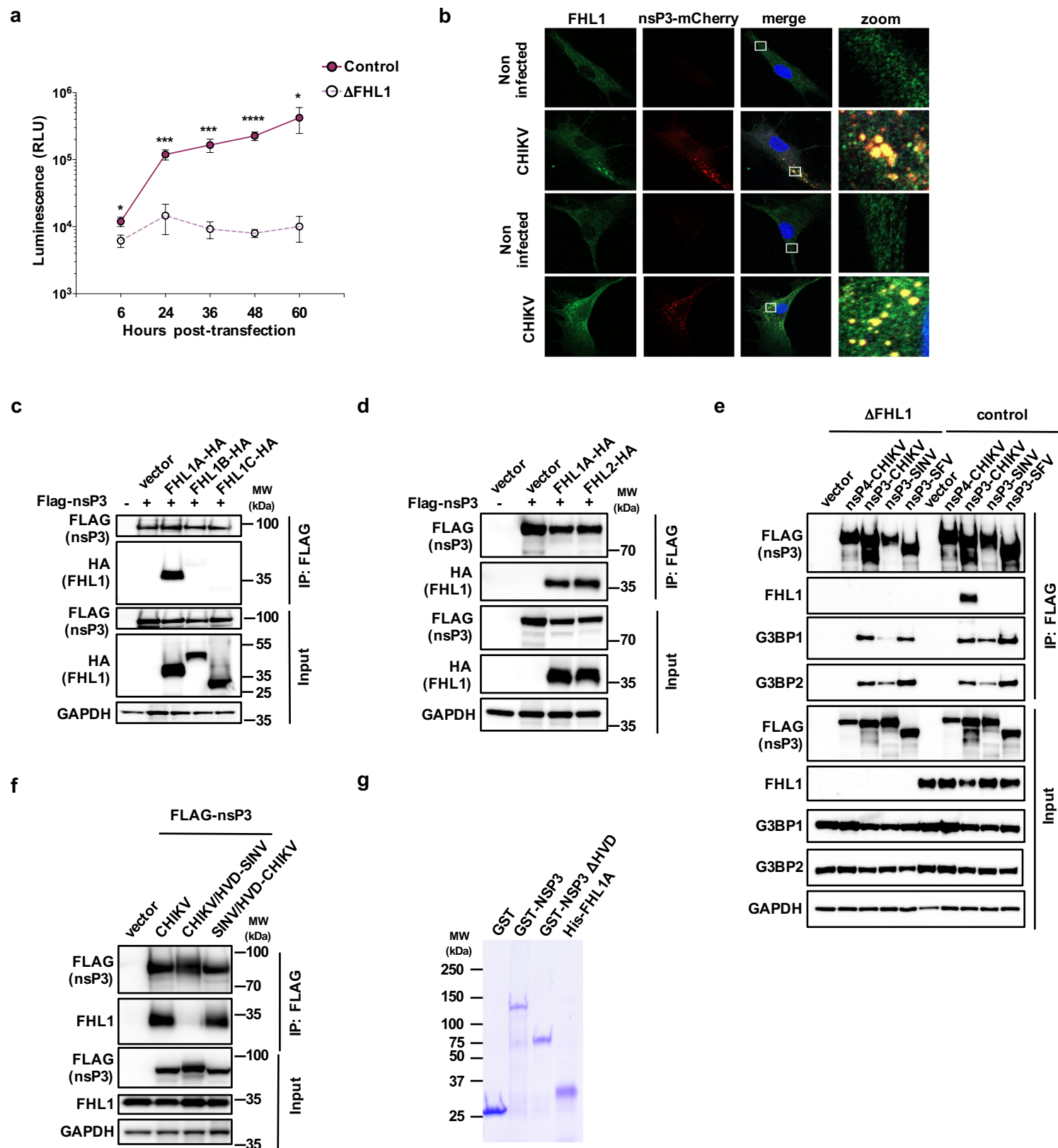




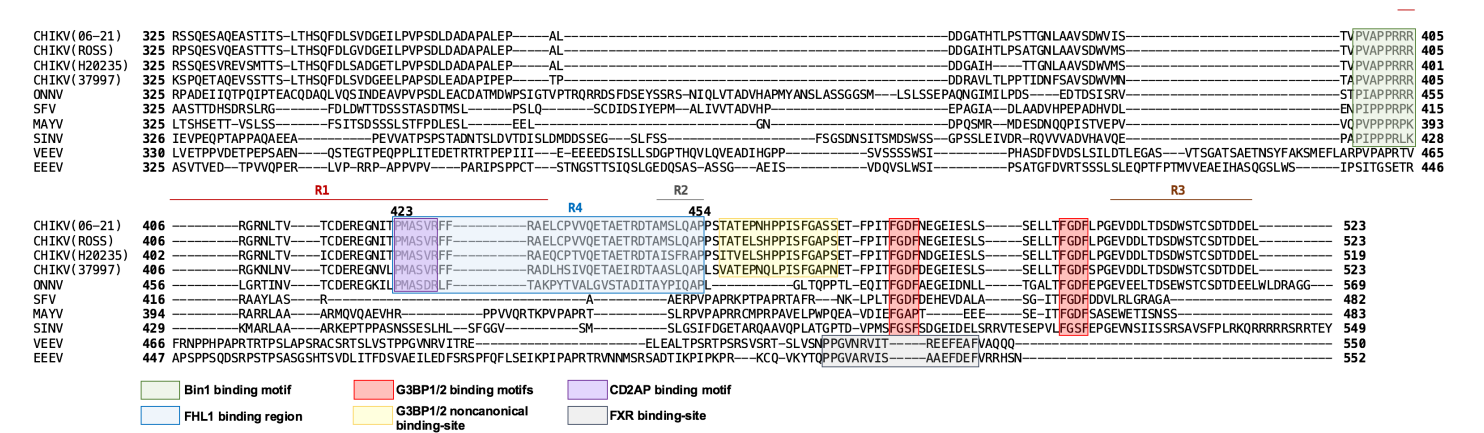




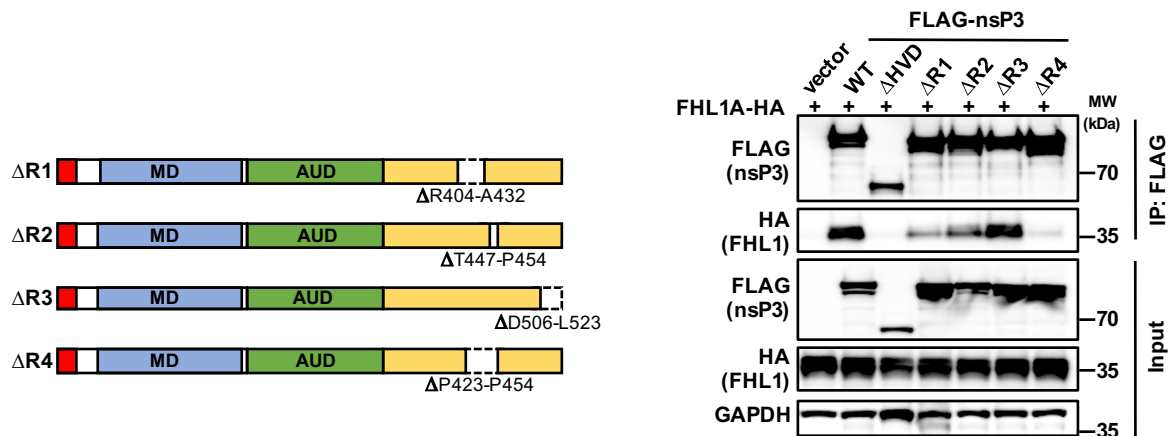
**a****b****c****d****e**



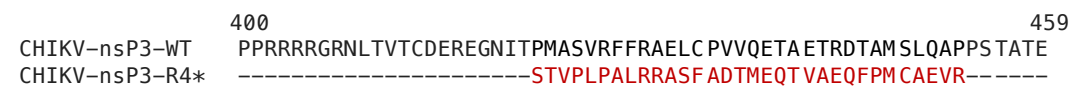
a



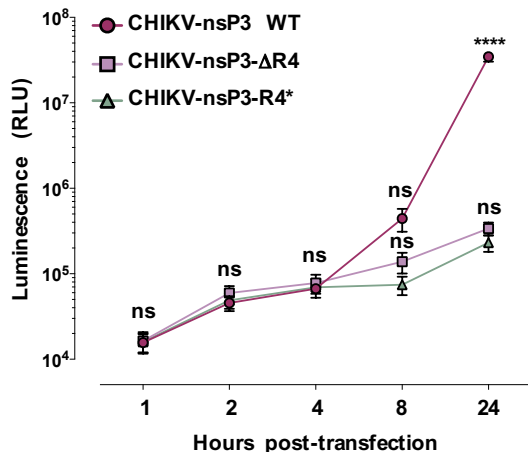
b



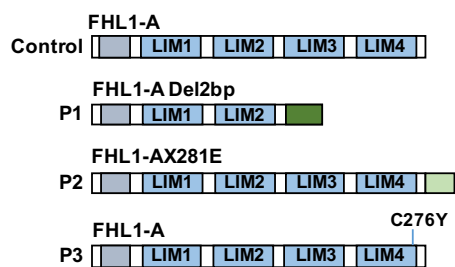
c



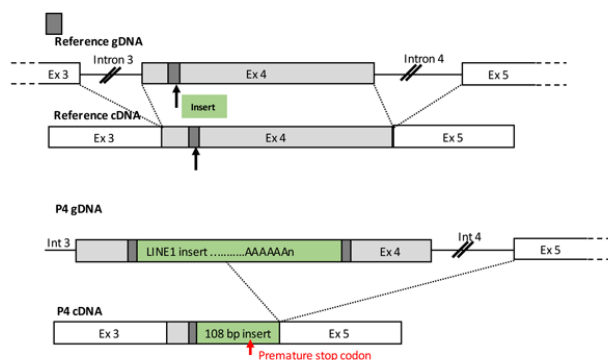
d



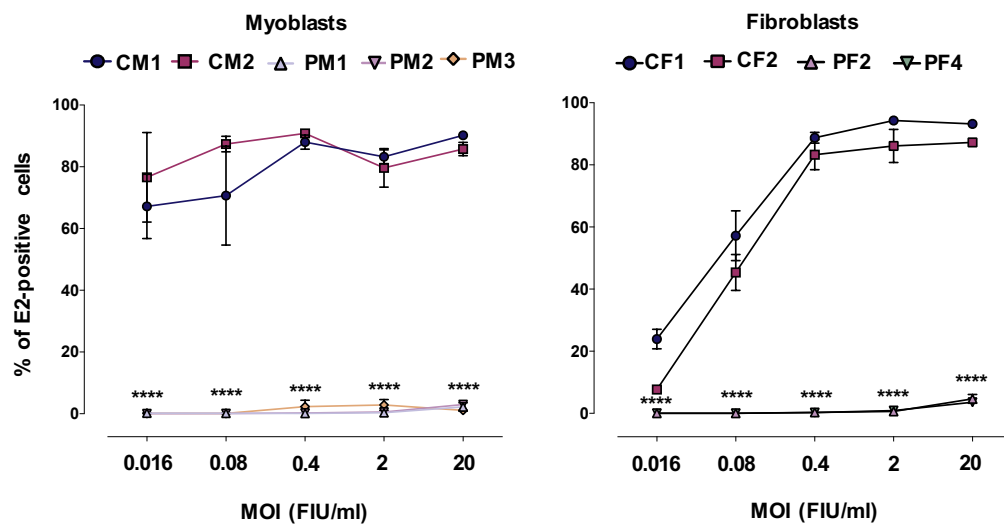
a



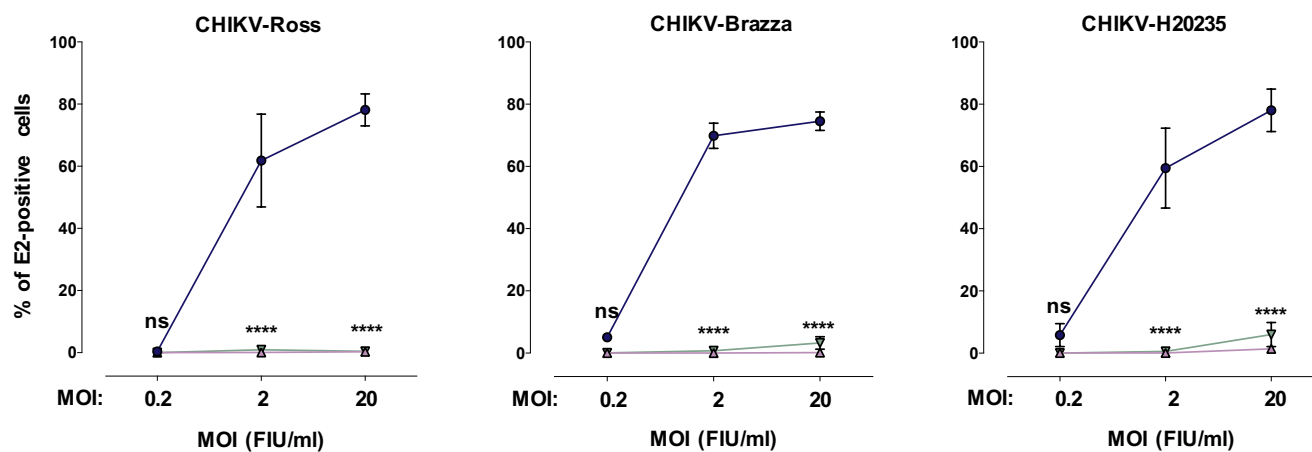
b



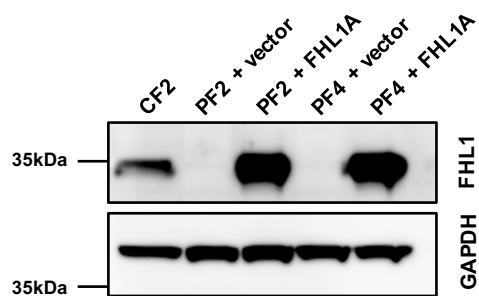
c



d



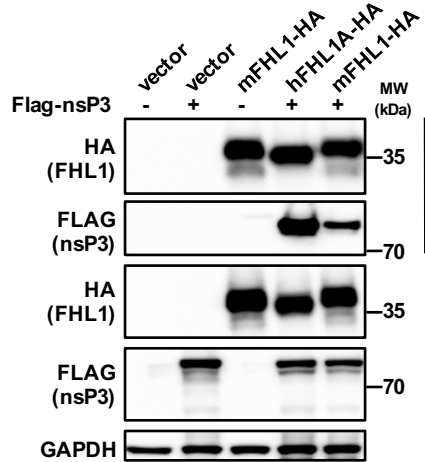
e



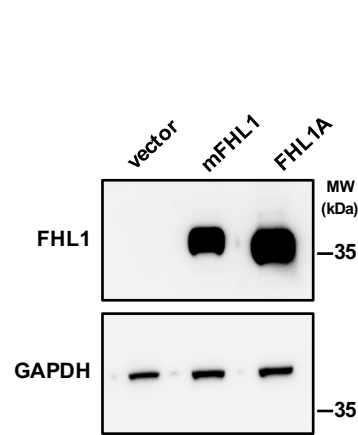
a

Human FHL1A	-----MAEKFDCHYCRDPLQGKKYVQKDGRHHCCLKCFDKFCANTCV <del>ECR</del>	44
Murine FHL1	MASQRHSGPSSYKVGTMSEKFDCHYCRDPLQGKKYVQKDGRHHCCLKCFDKFCANTCV <del>DCR</del>	60
Human FHL1A	KPIGAD <del>S</del> KEVHYKNRFWHD <del>T</del> CFRCAKCLHPLANETFVA <del>K</del> DNKILCNKCTREDSPKCKGC	104
Murine FHL1	KPI <del>S</del> AD <del>A</del> KEVHYKNRYWHD <del>N</del> CFRCAKCLHPLA <del>S</del> ETFVS <del>K</del> DGKILCNKCA <del>T</del> REDSPRCKGC	120
Human FHL1A	FKAIVAGDQNV <del>E</del> YKGT <del>V</del> WHKDCFTCSNCKQVIGTGSFFPKGEDFYCVTCHETKFAKHCVK	164
Murine FHL1	FKAIVAGDQNV <del>E</del> YKGT <del>V</del> WHKDCFTCSNCKQVIGTGSFFPKGEDFYCVTCHETKFAKHCVK	180
Human FHL1A	CNKAITSGGITYQDQ <del>P</del> WHA <del>D</del> CFVCVTCSSKLAGQRFTAVEDQYYCVDCYKNFVAKKCAGC	224
Murine FHL1	CNKAITSGGITYQDQ <del>P</del> WHA <del>E</del> CFVCVTCSSKLAGQRFTAVEDQYYCVDCYKNFVAKKCAGC	240
Human FHL1A	KNPITGFGKGSSV <del>V</del> AYEGQSWHDYCFHCKKCSVNLANKRFV <del>F</del> HQEQVYCPDCAKLL	280
Murine FHL1	KNPITGFGKGSSV <del>V</del> AYEGQSWHDYCFHCKKCSVNLANKRFV <del>F</del> HNEQVYCPDCAKLL	297

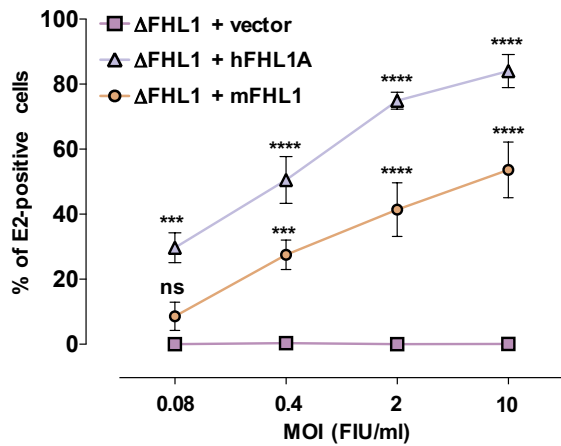
b



c



d



e

